



저작자표시-비영리-변경금지 2.0 대한민국

이용자는 아래의 조건을 따르는 경우에 한하여 자유롭게

- 이 저작물을 복제, 배포, 전송, 전시, 공연 및 방송할 수 있습니다.

다음과 같은 조건을 따라야 합니다:



저작자표시. 귀하는 원저작자를 표시하여야 합니다.



비영리. 귀하는 이 저작물을 영리 목적으로 이용할 수 없습니다.



변경금지. 귀하는 이 저작물을 개작, 변형 또는 가공할 수 없습니다.

- 귀하는, 이 저작물의 재이용이나 배포의 경우, 이 저작물에 적용된 이용허락조건을 명확하게 나타내어야 합니다.
- 저작권자로부터 별도의 허가를 받으면 이러한 조건들은 적용되지 않습니다.

저작권법에 따른 이용자의 권리는 위의 내용에 의하여 영향을 받지 않습니다.

이것은 [이용허락규약\(Legal Code\)](#)을 이해하기 쉽게 요약한 것입니다.

[Disclaimer](#)

Effects of part-to-part gap and the direction of welding on laser welding quality

The background features a large, light gray watermark of the UNIST logo. The logo consists of a circular emblem with a stylized 'U' shape in the center. Inside the 'U' is a globe with latitude and longitude lines. The text 'UNIST' is written in a bold, sans-serif font across the bottom of the emblem. The words 'UNIST NATIONAL INSTITUTE OF SCIENCE AND TECHNOLOGY' are written in a smaller, sans-serif font around the perimeter of the circle.

Hyun-Ki Kim

Engineering and Systems Design Program
Graduate School of UNIST

Effects of part-to-part gap and the direction of welding on laser welding quality

A thesis

submitted to the Graduate School of UNIST

in partial fulfillment of the

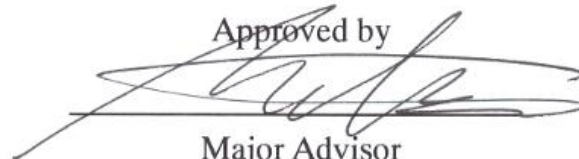
requirements for the degree of

Master of Science

Hyun-Ki Kim

02. 20. 2013

Approved by

A handwritten signature in black ink, appearing to read 'Duck-Young Kim', written over a horizontal line.

Major Advisor

Duck-Young Kim

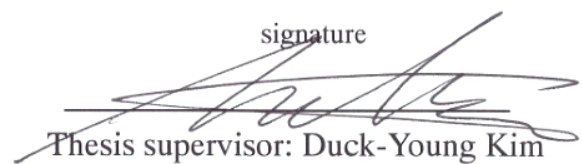
Effects of part-to-part gap and the direction of welding on laser welding quality

Hyun-Ki Kim

This certifies that the thesis of Hyun-Ki Kim is approved.

02. 20. 2013

signature



Thesis supervisor: Duck-Young Kim

signature



Nam-Hum Kim

signature



Hyung-Son Ki

Abstract

The use of laser welding has become quite widespread because it can achieve higher productivity than spot welding. This is due to its desirable features, which include high power density, faster welding speed, highly accurate welding, and excellent repeatability. In addition, laser welding can minimize the distortion in heat-affected zones (HAZs), and there is no tooling that wears out or must be changed over.

In spite of these advantages, laser welding still causes many problems when used on compositions such as galvanized steel and aluminum alloy. Galvanized steel, for example, is composed of a zinc layer whose physical parameters differ from those of steel as a base material. Zinc vaporizes at a temperature of 907 K, whereas steel begins to melt at 1510 K. This phenomenon causes serious defects in welds because the pressure of zinc is more powerful than that of steel. As a result, a certain manipulable control is needed in order for the zinc coating to be able to evaporate. To prevent this circumstance, the following solutions have been proposed: (i) a de-gassing method that induces the zinc fumes to escape from the part-to-part gap between two materials; (ii) the removal of zinc layers that will be joined together; (iii) a pulsed laser method that minimizes zinc vaporization using a high energy per pulse and a short pulse duration; (iv) a laser hybrid method; and (v) the addition of additional elements to the surface, which form a compound with the vaporizing zinc. Despite these suggestions, applications involving zinc-coated steels are rarely used in the automotive industry because the shapes of the materials to be welded are not always uniform.

In this study, we ascertain the effects of the part-to-part gap and the direction of welding on the quality of laser welding. Using a 2 kW fiber laser and galvanized steel sheets (with thicknesses of 1.4 mm and 1.8 mm), our experiments employed lap welding, which has been applied to side members in the automotive industry. The experimental design was used with a 3^3 factorial design with 3 replications. The three types of welding direction used are ascendance, descendance, and a uniform gap. Based on the experiments, using analysis of variance (ANOVA) it was determined that the direction of welding is an important factor that can affect the weld quality. In addition, the differences between the shear tensile strengths in the ascendance and descendance directions were determined using a t-Test. The maximum shear tensile strength in the ascendance direction was achieved with a laser power of 2000 W and a welding speed of 2100 mm/min, followed by a part-to-part gap of 0.32 mm/min as the steepest ascent method. Moreover, we analyzed cross-sections of sampling specimens, varying the gap differences in order to verify the differences in shear tensile strength based on two different directions of welding.

Contents

I. Introduction	1
1.1 Background	1
1.2 Motivation.....	4
1.3 Outline of the thesis	5
II. Literature survey.....	7
2.1 Principles of laser welding	7
2.2 Laser welding parameters	8
2.2.1 Laser-Related parameters.....	10
2.2.2 Process-Related parameters	11
2.2.3 Workpiece-Related parameter	12
2.3 Design of experiments and optimization.....	13
2.3.1 Design of experiments	13
2.3.2 Optimization	14
2.4 Real time monitoring	18
2.4.1 Optical detector.....	19
2.4.2 Acoustic detector.....	20
2.5 Part-to-part gap control	21
2.5.1 Physical gap control method	21
III. Experimental design.....	27
3.1 Laser welding system.....	27
3.2 Experimental material	30
3.3 Part-to-part gap	31
3.4 Direction of welding	32
3.5 Laser welding parameters	33
IV. Analysis of experiment.....	35
4.1 Analysis of Variance.....	35
4.2 Comparison between two different types of directions.....	38
4.2.1 t-Test.....	38
4.2.2 Steepest ascent method	39
4.3 Comparison of the shear tensile strength with directions of Ascendance and Descendance	44
4.4 Weld microstructure	47
V. Conclusion and future work	57

List of Figures

Figure 1.1.1: A classification of welding (Adopted from AWS)	2
Figure 1.1.2: Laser welding market in Korea (Kim, G.Y. 2011)	3
Figure 1.1.3: Remote laser welding of 3D scanner	4
Figure 2.2.1: Fishbone diagram for laser welding parameter optimization	9
Figure 2.2.2: Comparison of welding depth d versus welding speed v_w with experiments for 4 and 10 kW laser power (adopted from Kaplan)	11
Figure 2.4: Process signals during laser welding (Duely, 1999)	18
Figure 2.4.1: Typical setups for optical detectors using co-axial and off-axial arrangement	19
Figure 2.4.2: Typical setups for acoustic emissions.	20
Figure 2.5.1: Three types of de-gassing methods: (a) pre-drilled hole, (b) dimpling, (c) humping effect (Chen et al. 2009; Gu 2010; Hongping and Boris 2011).....	21
Figure 2.5.2: A schematic drawing of simplifying the concave model into the linear model	26
Figure 3.1.1: Principle of a laser (Sungwoo Hightech., Ltd).....	28
Figure 3.1.2: Optical dimensions of core diameter (adopted from Mazumder, 2010)	28
Figure 3.1.3: Fiber laser welding system (left) and welding with clamping (right)	29
Figure 3.2.1: Side member of a vehicle (SungWoo Hi-tech)	30
Figure 3.2.2: Shim gauge	31
Figure 3.2.3: A schematic drawing of lap welding of fiber laser welding.....	32
Figure 3.3.1: Schematic drawings of three types of laser methods	33
Figure 3.3.2: Hypothetical design of welded part based on the different types of welding	34
Figure 4.2.1: A schematic of First-order response surface and path of steepest ascent (Montgomery 2008)	39
Figure 4.2.2: Shear strength versus steps along the path of steepest ascent for direction of Ascendance (Welding speed: 2100 mm/min).....	42
Figure 4.3.1: Maximum shear tensile strength with 9 replications (Ascendance).....	45
Figure 4.3.2: Specimens breaks at base metals	47
Figure 4.4.1: Microstructures of SGARC440.....	48
Figure 4.4.2: Microstructures of SG AFC590DP.....	48
Figure 4.4.3: A schematic drawing of cross-sections arranged on the basis of their directions of welding.....	49
Figure 4.4.4: Cross-sections that had uniform gaps and exhibited the lowest strength (1) and the highest strength (2) in the entire experiment.....	51
Figure 4.4.5: Cross-sections that had a gap of 0.1 mm and exhibited the lowest strength: (1) Welded in the descendance and (2) ascendance	52
Figure 4.4.6: Cross-sections that had a gap of 0.1 mm and exhibited the highest strength: (1) Welded in the descendance and (2) ascendance	52
Figure 4.4.7: Cross-sections that had a gap of 0.2 mm and exhibited the lowest strength: (1) Welded in the descendance and (2) ascendance	53
Figure 4.4.8: Cross-sections that had a gap of 0.2 mm and exhibited the highest strength: (1) Welded in the descendance and (2) ascendance	53
Figure 4.4.9: Cross-sections that had a gap of 0.3 mm and exhibited the lowest strength: (1) Welded in the descendance and (2) ascendance	54
Figure 4.4.10: Cross-sections that had a gap of 0.3 mm and exhibited the highest strength: (1) Welded in the descendance and (2) ascendance	54
Figure 4.4.11: Cross-sections that had a gap of 0.32 mm and exhibited the highest strength: (1) Welded in the descendance and (2) ascendance	55
Figure 4.4.12: A comparison of the hypothesized (1) and experimentally determined results (2).	56

List of Tables

Table 3.1.1: Laser welding parameters	8
Table 2.3.1: Different methods of Design of Experiment and optimization.....	17
Table 2.5.1: The methods of alternatives creating gap	25
Table 3.1.1: A specification of fiber laser welding	29
Table 3.1.2: A specification of laser welding system at UNIST	29
Table 3.2.1: Chemical composition of galvanized steel sheets	30
Table 3.5.1: Experimental design of laser welding	33
Table 4.1: Design matrix with code process parameter and response parameter	35
Table 4.1.2: ANOVA table for 3 replication	36
Table 4.1.3: Experiment in Three Blocks	37
Table 4.1.4: ANOVA table for 3 replication in three blocks.....	38
Table 4.2.1: The results of t-Test from the two different directions of welding	39
Table 4.2.2: Process data for fitting the first-order model.....	40
Table 4.2.3: Analysis of variance for the first-order model (Ascendance)	41
Table 4.2.4: Steepest ascent experiment for the direction of Ascendance	41
Table 4.2.5: Process data for second first-order model	42
Table 4.2.6: Analysis of variance for the first-order model (Ascendance)	43
Table 4.3.1: Maximum shear tensile strength with 9 replications (Ascendance)	45
Table 4.3.2: Maximum shear tensile strength with 9 replications (Descendance)	46
Table 4.3.3: The results of t-Test from the two different directions of welding	46

I. Introduction

1.1 Background

Welding is a process that permanently joins metals, utilizing the different levels of interatomic penetration of those metals. Welding is carried out via the melting of workpieces by the introduction of intense heat, either while applying pressure or without applying pressure. In the act of welding, a filler material is also sometimes used.

On the basis of a survey of the literature and information from the American Welding Society (AWS), we can classify the welding process into seven different processes, which are shown in Figure 1.1.1. In a more general sense, these seven welding processes can be further categorized in three ways, as fusion welding, pressure welding, and soldering. Fusion welding, which is represented in the color red in Figure 1.1.1, takes place in the presence of a heat source, and makes use of filler material that can be in the form of a consumable electrode or a separate wire-feeding arrangement. Pressure welding takes place in the presence of mechanical pressure. Percussion welding, resistance welding, seam welding, and spot welding fall under the category of pressure welding. Soldering is a process in which two or more materials are joined together by melting the flow of a filler metal into the joint

In the automotive industry, gas metal arc (GMA), GMA brazing, alternating current metal inert gas (AC MIG), plasma MIG, and electron beam welding have been used for joining the parts of car bodies (Dilthey and Stein 2006; Hongping and Boris 2011). Nowadays, laser beam welding and remote laser welding are used in the body-in-white stage of vehicle manufacture.

According to the AWS, a variety of modern welding methods, such as hybrid laser/plasma arc welding, are being applied in industry worldwide. These modern welding processes are a better approach to increasing the productivity and quality of the weld, and a great deal of research is being conducted in this regard. This research was accelerated when the patent for the friction welding process expired in 2010. The efficient use of electricity also opened a broad area of research in the field of welding technologies.

Different energy sources are utilized in the welding process, including a gas flame, an electric arc, a laser, an electron beam, friction, and ultrasound. Welding may be performed in many different environments, including the open air, under water, and in outer space. Because welding can be hazardous, precautions must be taken to avoid burns, electric shock, vision damage, inhalation of poisonous gases and fumes, and exposure to intense ultraviolet radiation.

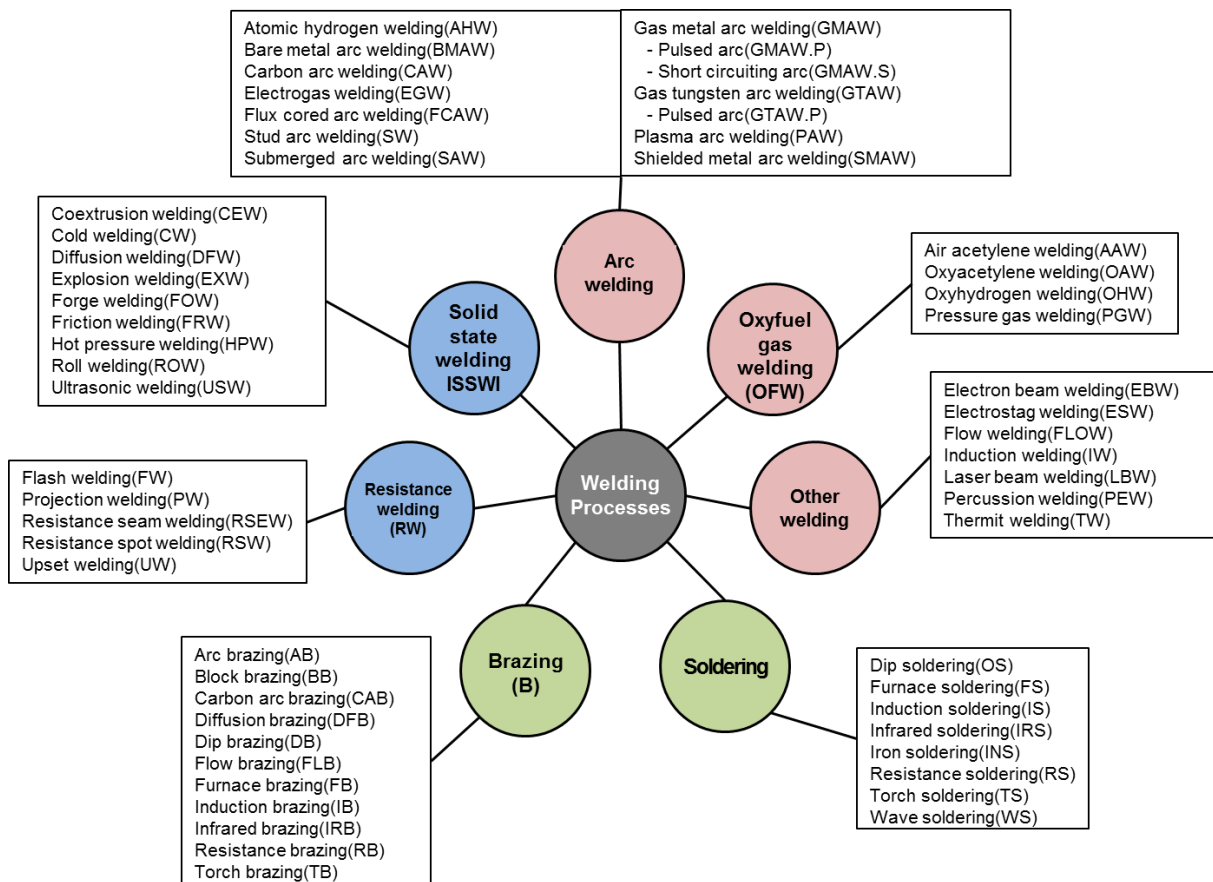


Figure 1.1.1 A classification of welding (Adopted from AWS)

Three decades ago, laser welding was an infant welding method that was used only in research applications. Recently, laser welding has been applied in the metalworking industry, where it can be used in place of other approaches, such as spot welding, submerged arc welding, and electron-beam welding. A focused laser beam is one of the highest density power sources available to industry; its power density is similar to that of an electron beam. The laser welding process represents a part of the new technology of high-energy-density processing (Steen and Mazumder 2010). Laser welding is also being applied in the automotive, aerospace, marine, and railway industries. In the automotive industry in particular, lasers are being applied in the manufacture of components such as cover bumpers, cross members, side members, pillars, etc. Laser welding has been quite widely used in the automotive industry because unlike spot welding, it can achieve high accuracy, excellent repeatability, and unit cost reduction. In addition, it can minimize the distortion in heat-affected zones (HAZs), has no tooling that wears out or must be changed over, and offers versatility in working with different materials. The disadvantages are that laser welding plants are expensive, and the filler materials that are used are also quite costly. There are also some health concerns involved, since a laser can damage

the eyes if one looks directly into it, and can cause serious burns if one's skin comes in contact with it.

In terms of the quality of weldment, industries in Korea tend to produce a lower quality than those in the United States and United Kingdom. The main reason for this lower quality is that only a few small industries have invested in related research and development. However, Korea's application of the technologies of laser welding is outstanding compared to that of other countries (Kim, K.Y. 2011). The scale of the welding monitoring market and inspection system market was 12.7 trillion dollars in 2008, and Korea captured 4% of this. In addition, weld seam tracing and inspection of a bead profile using optic sensors and acoustic emission (AE) have been developed.

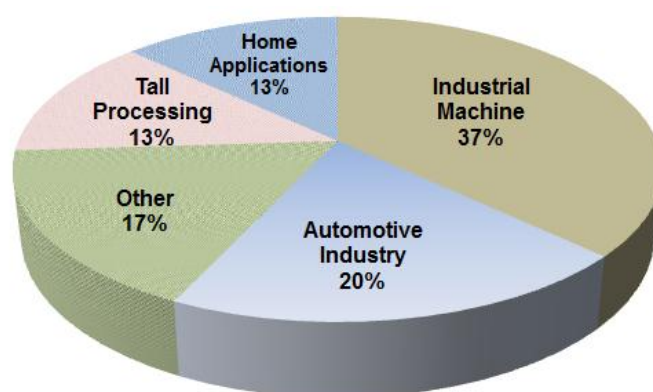


Figure 1.1.2 Laser welding market in Korea(Kim, G.Y. 2011)

In the global market, the trends in laser welding are moving in the direction of high power, high efficiency, high beam quality, and a long life span based on green energy concepts. Germany, France, and the United Kingdom are the world leaders in the production of laser technologies, and Germany has even developed a laser combination-head that can weld and cut at the same time (Kim, K.Y. 2011).

Remote laser welding is different from conventional laser welding because the beam is conducted to the work surface via small lightweight mirrors, instead of a conventional focusing head (Klingbeil 2006). This form of welding uses scan mirrors in order to position the beam accurately on the target weld location. Nowadays, remote laser welding is provided with 3D scanners that can operate on the X, Y, and Z axes automatically. Figure 1.1.3 shows a 3D scanner with 3 axes. With the use of this kind of scanner, the positioning speed can be decreased so that the welding speed can be increased.

Unlike the work head used in conventional laser welding, remote laser welding is conducted at a

distance from the workpiece, which makes it possible for the working hours to be reduced and high efficiency to be achieved. Moreover, the welding head and scanner are adapted for installation on welding robots that just move along the detailed weld parts. The focal length of remote laser welding is greater than 500 mm, which is a longer distance than can be achieved using the conventional method. Currently, the only lasers that satisfy this criterion are fiber lasers, disk lasers, and CO₂ lasers (Kim et al. 2005).

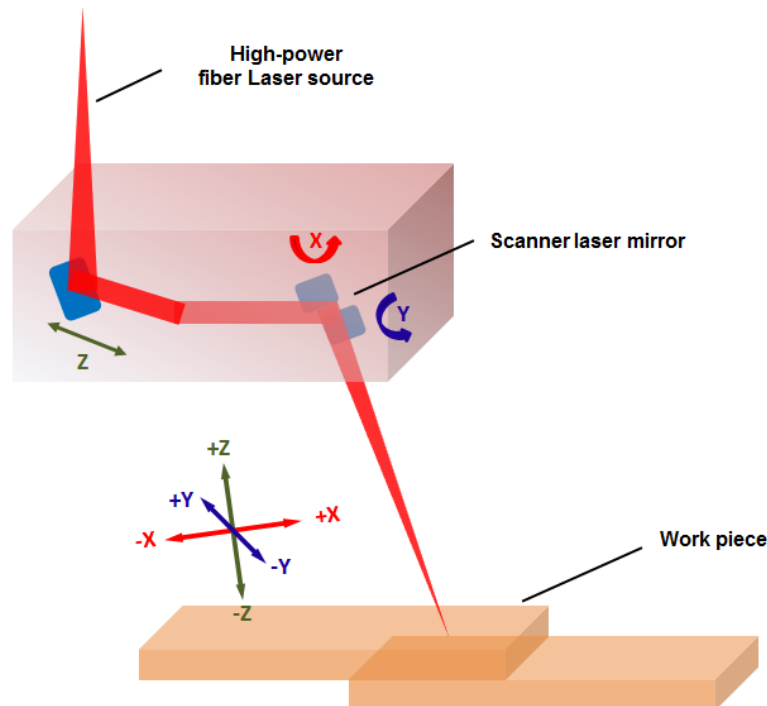


Figure 1.1.3 Remote laser welding of 3D scanner

1.2 Motivation

Galvanized steel has very high corrosion resistance. The enormous usage of thin steel sheets in automotive applications to reduce the weight of a vehicle makes it essential to improve the material strength as well as provide higher corrosion protection. Hot dip galvanizing of steel sheets is known as a powerful technique to protect against oxidation, and thus failure due to corrosion (Katundi et al. 2010). For automotive parts in particular, two main welding methods are used: lap welding and butt welding.

In spite of these advantages, laser welding with compositions such as galvanized steel and aluminum alloy still causes many problems. In the case of galvanized steel, it is composed of a zinc layer whose physical parameters differ from those of the steel that serves as a base material. Zinc

vaporizes at a temperature of 907 K, whereas steel begins to melt at 1510 K. This discrepancy causes serious defects in welds because the pressure of zinc is more powerful than that of steel. As a result, a certain manipulable control is needed in order for the zinc coating to be able to evaporate. To prevent this circumstance, the following solutions have been proposed: (i) a de-gassing method that induces the zinc fumes to escape from the part-to-part gap between two materials; (ii) the removal of zinc layers that will be joined together; (iii) a pulsed laser method that minimizes the zinc vaporization using a high energy per pulse and a short pulse duration; (iv) a laser hybrid method; and (v) the addition of additional elements to the surface, which form a compound with the vaporizing zinc. Despite these suggestions, applications involving zinc-coated steels are rarely used in the automotive industry because the shapes of the materials to be welded are not always uniform.

In this study, we ascertain the effects of the part-to-part gap and the direction of welding on the quality of laser welding. Using a 2 kW fiber laser and galvanized steel sheets (with thicknesses of 1.4 mm and 1.8 mm), our experiments employed lap welding, which has been applied to side members in the automotive industry. The experimental design was used with a 33 factorial design with 3 replications. The three types of welding direction used are ascending, descending, and a uniform gap. Based on the experiments, using analysis of variance (ANOVA) it was determined that the direction of welding is an important factor that can affect the weld quality. In addition, the differences between the shear tensile strengths in the ascending and direction of descendance were determined using a t-Test. Moreover, we analyzed cross-sections of sampling specimens, varying the gap differences in order to verify the differences in shear tensile strength based on two different directions of welding.

1.3 Outline of the thesis

This thesis is organized as follows. Chapter 2 provides a review of the literature related to laser welding gap control. In Chapter 3, an experimental laser welding system is introduced, and experimental materials and an experimental design are suggested. Chapter 4 shows the results of the experiments, and determines the optimal region in which maximum strength can be obtained, based on the direction of the weld. Chapter 5 presents a discussion in which the results are analyzed in order to corroborate our intents. Finally, Chapter 6 presents our conclusions and suggests a course of future study.

This Page Intentionally Left Blank

II. Literature survey

In this chapter, a detailed survey on part-to-part gap control related laser welding. Firstly, general principles of laser welding are introduced. Secondly, laser welding parameters are classified according to the laser related parameter, process related parameter, and work piece related parameter. Thirdly, related researches with part-to-part gap control are described depending on the alternatives of creating gap, monitoring, and numerical optimization.

2.1 Principles of laser welding

Laser emission at optical wavelengths was first reported in 1960 with the announcement of laser oscillation in optically pumped ruby crystals. By 1962, there had been several reports on metallurgical applications of lasers including welding. This was followed by a number of fundamental studies of laser welding. The advantages of laser welding in comparison to soldering of fine wires and electronic components were soon realized.

Basically, laser has three main components called gain medium, pumping source, and resonator. Gain medium contains atom which emit monochromatic light (laser light) when excited by fed-in energy. Pumping source is to deliver the required pump energy to excite the atoms of the laser medium. Resonator is comprised of a high-reflecting and a partly permeable mirror. So, laser medium is between the mirrors. The optical resonator, or optical cavity, in its simplest form is two parallel mirrors placed around the gain medium which provide feedback of the light. The mirrors are given optical coatings which determine their reflective properties. Typically one will be a high reflector, and the other will be a partial reflector. The latter is called the output coupler, because it allows some of the light to leave the cavity to produce the laser's output beam.

Some of the advantages of laser welding are: (Duley 1999; Steen and Mazumder 2010)

- Deep narrow welds are obtained easily, even eliminating the addition of filler material and the need of a V joint preparation.
- Low heat input and high power density in the work piece, producing very low thermal distortion and small heat affected zones (HAZ) avoiding the risk of excessive grain growth.
- High welding speeds can be used, permitting high production rates.
- The process flexibility is high, welding can take place in all laser beam positions and laser can be easily automated if the beam is delivered by fiber optics (not possible for CO₂ lasers).

- Laser welding improves component design opportunities, high thickness materials can be welded, a wide range of joint configurations can be used and it reduces considerably the post weld machining processes.

On the other hand the main disadvantages of this technology are:

- Small joint gaps and well clamped joints are required. The laser beam focused is really narrow and it can pass through small gaps. Also, poorly fitting parts produce undercut welds.
- An accurate beam and joint alignment is needed.
- Safety protections are essential, the equipment needs to be maintained on a stable base to avoid vibrations and it is not equipment with good portability.
- Equipment and operation costs are high compared to other conventional welding methods.

2.2 Laser welding parameters

In general, focus length, focus position, and focus size are playing an important role in a laser welding because it is a welding method using a light with high and tiny spot. Laser welding is mainly divided from 3 parameters: laser-related parameters, process-related parameters and workpiece-related parameters (Table 3.1.1) (Cao et al. 2003).

Table 3.1.1 Laser welding parameters

Laser-Related Parameters	Process-Related Parameters	Workpiece-Related Parameters
Wavelength	Welding Speed	Composition
Laser Power	Shield Gas	Thickness
Spot Size	Filler Metal	Surface Condition
Focal Length		Joint Design and Fit-up
Depth of Focus		Fixturing
Focal Plane Position		
Beam Alignment		
Multi-beam Technique		
Beam Spinning and Weaving		

To become narrower for our interest of study, fishbone diagram is necessary. A fishbone diagram is a useful way to organize information related to our purposes. In Figure 2.2.1, two main parameters are divided. Uncontrollable parameters are shown that environment like humidity or temperature is out of our capacity. On the other hand, controllable parameters are that we can control parameters are arranged. In addition, laser-related parameters, process-related parameters and workpiece-related parameters can belong to the controllable parameters. Bottom section of the fishbone diagram is composed of methods and inspections. Optimization methods and design methods are the representative ways of the method and there are two main inspections: destructive inspections and non-destructive inspections. When parameters and methods are arranged, desirable laser welding parameters optimizations will be achieved.

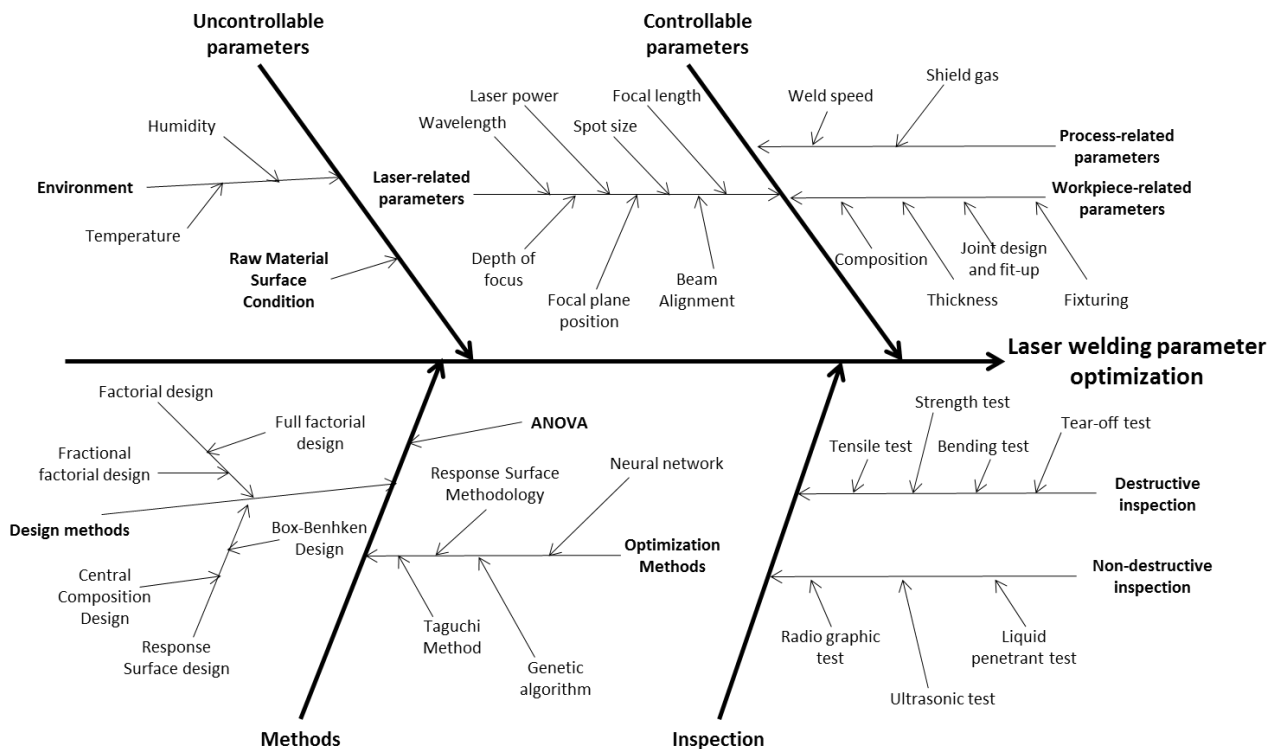


Figure 2.2.1 Fishbone diagram for laser welding parameter optimization

2.2.1 Laser-Related parameters

Wave length

Reflectivity of laser beam is the ratio of reflection on incident surface and the value has '0', '1'. From this value, the value of input energy can be estimated when processing materials.

$$R = 1 - k\left(\sigma \frac{\lambda}{c}\right)^{-1/2} \quad (1)$$

k: a constant related to the material, λ : wave length of laser beam

σ : conductivity of materials, c : the speed of light

From the equation (1), the reflectivity will increase when the wave length is increase. Thus, decision of selecting a wavelength of laser beam is important.

Laser power

Laser power is a crucial parameter when investing the limits of welding depth. If laser power is too low, two materials cannot be jointed due to the low heat input. When laser power is too high, some defects are detected such as spatters, under-cut, under-fill, and drop-out. In addition, laser power should be set up depends on the different material (Kaplan et al. 2009).

Spot size

Spot size is an important parameter related to the laser power. The equation of spot size is following,

$$W_0 = (\lambda \times f) / (\pi \times W_L) = f \times \theta_{ff} \quad (2)$$

W_L : reflected beam diameter

From the same laser power, smaller spot size has higher power density so that weld width should be narrow and weld penetration should be deeper. However, when spot size is too small, which means too high density, under-cut or under-fill can be occurred (Cao,Wallace et al. 2003).

Focal length

Focal length is strongly related to the depth of focus which is a tiny point that can be limited allowable range (Cao,Wallace et al. 2003). When focal length becomes short, beam waist diameter and depth of focus are decreased, whereas the convergence angle is increased. Too short focal length can cause some problems to the lens with spatter and vapor damage. Too long distance of focal length brings about the oxidation on the root weld from materials (Larsson et al. 2000).

Operational mode

Operational mode can be divided from pulsed wave (PW) and continuous wave (CW). Generally CW is used for the high-speed welding and PW is used for the precise welding (IPG Photonics ; Kelkar 2008). The good beam quality of the fiber lasers coupled with high CW powers offers deep penetration. Modulating these CW lasers offer pulsed laser capabilities with high peak and low average power for low heat input applications (IPG Photonics). When welding with aluminum alloy, pulsed wave is contributed to the better weldability, which results that pulsed wave welding can weld deeper penetration than continuous wave welding(Cao,Wallace et al. 2003).

2.2.2 Process-Related parameters

Welding speed

Welding speed is a speed at which the weld is created over the workpiece and it is commonly measured in m/min or mm/sec (ANSI/AWS 2001). Welding speed is related to the laser power, material, and welding depth. Based on the same laser power, weld depth is decreased when welding speed is increased (Kaplan,Norman et al. 2009) as shown in Figure.2.2.2. Also, depends on the types, characteristics, and thickness of materials, welding speed should be different.

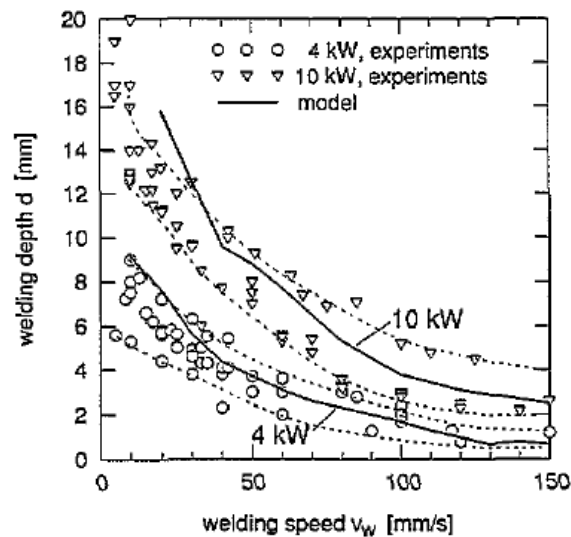


Figure. 2.2.2 Comparison of welding depth d versus welding speed v_w with experiments for 4 and 10 kW laser power (adopted from Kaplan).

Shield gas

Shield gas protects high molten materials from the oxidation so that it plays a role in preventing from nonmetallic inclusions of oxides and formation of porosity (Kim and Kim 2007). Plasma or plume formation via the release of vaporized material from the keyhole must also be suppressed, especially in CO₂ laser welding because it can cause instabilities of the vapor-filled keyhole, reduce weld penetration, produce coarse porosity, and reduce life of coverglass slides (Cao,Wallace et al. 2003). Also, lack of shield gas can occur porosity, undercut, and bead roughness (Cao,Wallace et al. 2003).

Filler metal

Filler metal is a compensation for the top and bottom bead using additional metal. Using filler metal, the chances such as porosity and hot cracking can be decreased and make plasma vapor stable states (Larsson,Palmquist et al. 2000). In addition, the angle of filler metal which is provided with to the beads plays an important role in absorbing the energy. However, too high feed rate can interrupt the full penetration on the bottom or top beads (Cao,Wallace et al. 2003).

2.2.3 Workpiece-Related parameter

Composition

Volatile compositions such as magnesium, zinc, lithium, and aluminum tend to melt easily compared to the steels. When these materials are welded, because of relatively low melting point and high pressure, many welding qualities are discussed and suggested. Also, these compositions can be strongly affected by laser density and welding speed.

Thickness

Thickness of materials should be set up based on the type of materials. This is because each and every material has its own welding depth and this welding depth should be related to the laser density and welding speed. In other words, thicker materials should be high power laser density and low welding speed(Cao,Wallace et al. 2003).

Surface condition

Generally metal has high reflexivity to the light. Especially high electric conductive materials such as aluminum and copper have high reflexibilities so that it makes laser process difficult due to the bad heat efficiency. Also, the same materials but different surface condition can affect negative results because each material has different reflexivity (Zhao et al. 1999).

2.3 Design of experiments and optimization

The Design of experiments (DOE) is the process of planning the experiment so that the appropriate data will be collected and analyzed by a statistical method, resulting in valid and objective conclusions (Montgomery 2008). For the laser welding, we need to have design of experiments with careful considerations because laser welding system is expensive to use. For this reason, factorial design, response surface methodology, and Taguchi method have applied in order to obtain the crucial information with minimum number of experiments.

2.3.1 Design of experiments

Factorial design

k^n factorial design is composed of n factors and k levels. It also has factorial experiment that can estimate all kinds of factorial effects. By a factorial design, we mean that in each complete trial or replication of the experiment all possible combinations of the levels of the factors are investigated (Montgomery 2008).

From the manufacturing industries, the laser welding process was conducted using resolution IV fractional factorial design, with the I=ABCD by Tanco. In this research, the purpose is to improve a laser welding process in a one-model car production line. He suggested that the input parameters, such as power, current, clearance of side, and clearance of the roof could affect the surface of the side being used in the factorial design. From that result, the defects of the side decreased to the 97 percentage, so that it achieved cost reduction (Tanco et al. 2008).

Khan (2011) reported an experimental design approach to process parameter optimization for the laser welding of martensitic AISI 416 and AISI 440FSe stainless steel lap welding with 0.55mm thickness. His research is to develop mathematical models for all response factors of the weld and determine the optimal range of welding parameters that minimize the weld width and maximize the weld penetration depth, weld resistance length, and weld shearing force. He described that laser power and welding speed was the most important factors to the bead profiles using full factorial design. He also concluded that proper laser power and welding speed can decrease a weld width and increase the penetration depth so that resistance length and shearing force will be increased (Khan et al. 2011).

Park (2010) reported that there is some strength degradation when welding with AA5000 series. In order to protect from this degradation, filler wire is carried out and weld formability is predicted using factorial design and regression model. In this research, 3^3 factorial design was used, groove 'I type' butt welding was carried out. The weldability estimation was from the Erichsen test and he

developed the predicted model using regression model (Park 2010).

Gunaraj (1999) used submerged arc welding (SAW) in order to find optimal parameter for the bead quality. For the experimental design, 2^4 factorial design was run with 7 center points and 8 star points. From these experiments, he suggested that penetration depth, reinforcements, and weld width were decreased when welding speed was increased. However, despite the increase of wire filler rate, penetration depth, reinforcement, and the percentage dilution of the weld bead were increase except weld width (Gunaraj and Murugan 1999).

2.3.2 Optimization

Response surface methodology

Response Surface Methodology (RSM) is a collection of statistical and mathematical techniques useful for developing, improving, and optimizing process. It also has important applications in the design, development, and formulation of new products, as well as in the improvement of existing product design (Myers et al. 2009).

Response surface methodology for the laser welding is mainly divided bead profile, strength, and stress analysis. Benyounis (2005) reported the optimization of laser-welded butt joints of medium carbon steel sheet using RSM. He used a Box-Behnken design with 3 level and 3 factors and his optimization method is consist of numerical optimization and graphical method. Numerical optimization has two separate ways which are the goal of half and full penetration. Graphical optimization is to show some optimal criteria with certain limits. He suggested that full depth penetration strongly affects the other bead parameters. In addition, strong, efficient, and low cost weld joints could be achieved using the optimum welding conditions (Benyounis et al. 2005).

Benyounis also reported a paper about the optimization of medium carbon steel on the bead profile which is composed of heat input, penetration depth, weld width, HAZ width. Using RSM, he deducted the second order equation and analyzed the relationships between laser parameters and bead profile parameters. From this result, laser power has a positive effect, while welding speed has a negative effect and heat input plays an important role in the weld-bead parameters dimension (Benyounis et al. 2005).

His different research is to reduce the joint-operating cost with multi-response optimization of laser welding process of austenitic stainless steel. From this experiment, welding speed is the most important parameter and the optimal input parameter is when laser power is 1.2 ~ 1.23 kW. Moreover, from the optimization, it is possible to achieve almost 43 percentage of the cost reduction (Benyounis

et al. 2008).

Olabi suggested that the best combinations of parameters that minimized the stress in the heat affected zone using RSM, factorial design, Taguchi method, and numerical algorithm. From the experiment, low laser power, high welding speed, and intermediate focus point position were carried out the minimizing the residual stress. In addition, stress was rarely affected by the focus position and welding speed strongly affected the residual stress (Olabi et al. 2007).

Acherjee reported a prediction of weld strength and seam width for laser transmission welding of thermoplastic using RSM. From RSM, he described the relationships between laser parameters and output parameters, so each an equation of lap-shear strength and weld-seam width was carried out using regression model and showed the interaction graphs between laser parameters and output parameters. For lap-shear strength, when laser power is increased, shear strength and weld width is increased. From the Stand-off distance, when stand-off distance is increased, weld width is following the stand-off distance. However, clamp has only slight positive effect on the shear strength. Also, welding speed strongly affect the shear strength and welding speed and weld width (Acherjee et al. 2009).

Zhao reported the optimal parameter of laser welding thin-gage galvanized steel using RSM. In this paper, crucial thing is to use 0.4mm thin gage which is less than 0.6mm. Also, his conduction is to measure the maximum penetration depth based on the half penetration. He carried out the three levels and four factors with a uniform design proposed by Fang and Wang in 1980's. From the experiment, there are severe spatter and porosity in the weld when using 4mm-thick galvanized SAE1004 steel sheet without any gap. Also, the optimal parameters is when laser power is 628W, welding speed is 34.7mm/s, gap is 0.12mm, and defocus amount is -0.23mm (Zhao et al. 2012).

Gunaraj reported an application of RSM for predicting weld bead quality in submerged arc welding of pipes. He used a titanium alloy with 1.7mm thickness and CO₂ laser welding system. He considered five response parameters (weld width, HAZ, welded zone area, HAZ area, and penetration depth) and find out the optimal parameters using regression model. He suggested that 1837.4 of laser power, 25.4 mm/s of welding speed, and 0.6941mm of focal position were the optimal parameters for obtaining the best bead geometry produced from Titanium alloy. In addition, welding speed has a negative effect on all response, whereas laser power has positive effect on response parameters. Lastly, focal position has no effect on bead geometry of titanium alloy (Gunaraj and Murugan 1999).

Taguchi method and Artificial Neural network

Taguchi method is one of the optimization methods that applied to the laser parameters. One of the advantages of Taguchi method is to achieve high quality without increasing the cost (Anawa and

Olabi 2008). The power of the Taguchi method is in its clarifying the dominant factor given the complex interaction which occur in laser welding, involving the shielding gas, laser power, welding speed, focus position, and pulsed frequency (Pan et al. 2005).

Artificial Neural Network (ANN) model is developed to select welding parameters such as laser power, welding speed, focal position and focal length for required output parameters such as penetration depth, weld width, and HAZ width. For optimization method in laser welding field, Taguchi method and ANN usually used together.

For laser welding, Taguchi method has applied in order to control the laser parameters appropriately. Olabi suggested an ANN and Taguchi algorithms integrated approach to the optimization of CO₂ laser welding. For the goal to maximize penetration-to-fuse-width and the penetration-to-HAZ-width ratio, Taguchi L₉ design was used and ANN was designed in order to calculate penetration-to-fuse-width and the penetration-to-HAZ-width for different laser powers, welding speeds, and focal positions (Olabi et al. 2006). He also used

For the optimization fields, Olabi (2006) used a Taguchi method and Artificial neural network to find optimal parameters using CO₂ laser welding with thickness of 5mm medium carbon steel sheets. He suggested that 1.42 of laser power, 50cm/min of welding speed, and 2.5mm of focused position are the optimal parameters (Olabi,Casalino et al. 2006). He also suggested optimal parameters in order to minimize residual stress using response surface methodology using CO₂ laser welding. In this research, he used butt welding on stainless steel sheets and optimal parameters are 1.15 to 1.22kW of laser power, 55 to 50cm/min and -0.8mm of focal point position (Olabi et al. 2007). Moreover, he reported three optimization methods for laser process in order to minimize residual stress in the heat affected zone. Using CO₂ laser welding with 3mm thickness of stainless steel, he compared three kinds of optimization methods, Taguchi method, Response surface methodology, factorial design, and numerical algorithm. 1.03kW of laser power, 68.52 cm/min, and -0.5mm of focused position were set up comparing with residual stress (Olabi,Casalino et al. 2007).

Benyounis (2005) suggested the optimal parameters of the heat input and weld-bead profile using response surface methodology. He tried to describe some relationship among the input parameters and output parameters by using developed models. Desirable parameters are 1.2 to 1.43kW of laser power, 30 to 70 cm /min and -2.5 to 0 focal point position when welded 5mm thickness of medium carbon steel sheets0 (Benyounis,Olabi et al. 2005). He also studied multi-response optimization of austenitic stainless steel with CO₂ laser welding. He used 3mm thickness of austenitic stainless steel sheet and between 1.2 and 1.23kW of laser power and between 35 and 39cm/min of welding speed with -0.2 mm of focus position(Benyounis,Olabi et al. 2008). Anawa3 (2008) reported optimal parameters using Taguchi method. In this study, CO₂ laser welding was used and butt welding method of stainless steel

and milled carbon steel was carried out. He suggested that welding speed can be the most important parameter for strength of welded pool (Anawa and Olabi 2008).

Pan (2005) used a Taguchi method in order to optimize the laser parameters which affect the tension stress when butt welding onto magnesium alloy. Various combinations were considered to evaluate the relative importance of welding parameters. From this paper, optimal combination of welding parameters is Argon shielding gas, 360W for laser power, 25mm/s for welding speed, 160Hz for the pulse frequency. Also, ultimate tension stress was maximum at an overlap of the welding zone of approximately 75% (Pan,Wang et al. 2005).

Table. 2.3.1 Different methods of Design of Experiment and optimization

Design method	Control parameter	Quality measurement	Experimental design	Related work
Screening (Factorial design)			- 3 ³ full factorial design - 2 ⁴ fractional factorial design	(Gunaraj and Murugan 1999; Benyounis,Olabi et al. 2005; Olabi,Casalino et al. 2007; Park 2010; Khan,Romoli et al. 2011)
Response surface methodology (Optimization)	- Laser power - Welding speed - Focused position - Focal length - Shielding gas - Pulse frequency - Wire feed rate - Nozzle to plate distance - Clamp pressure - Gap - Spot size	- Penetration depth - Bead width - Bead Width area - HAZ width - HAZ width area - Tensile strength - Impact strength - Lap-shear strength - Residual stress - Joint cost - Erichsen value - Reinforcement - Dilution - Heat input	- Box-Behnken design(BBD) - Central Composition Design(CCD) - Uniform design	(Gunaraj and Murugan 1999; Benyounis,Olabi et al. 2005; Olabi,Benyounis et al. 2007; Olabi,Casalino et al. 2007; Benyounis,Olabi et al. 2008; Acherjee,Misra et al. 2009; Khorram et al. 2011; Zhao,Zhang et al. 2012)
Taguchi (Optimization)		- Focused position - Weld-seam width - Concave	- Orthogonal arrays	(Pan et al. 2004; Yoo et al. 2006; Olabi,Casalino et al. 2007; Anawa and Olabi 2008)
ANN (Optimization)			- Orthogonal arrays	(Son et al. 1999; Olabi,Casalino et al. 2006)

2.4 Real time monitoring

Before high power laser was invented, laser-induced plasma has been huge experimental and theoretical researches ([Hafeez et al. 2008](#)). In general, when laser welding is operated, a plume is accompanied under the conduction-limited conditions. The plume is the result of the ejection of material from the area of the weld because of laser beam ([Duley 1999](#)).

As plasmas signal vaporization and, specifically, the interaction between vaporized material and an incident laser beam, the information obtained through analysis of plasma radiation is only indirectly related to the laser material interaction that results in welding. The use of plasma diagnostics in monitoring laser welding then relies on the availability of a model that relates the observed variable to some aspect of the weld condition.

Optical and acoustical process signals can be measured from the emissions of the welding using suitable sensors. Signals have information on the beam-material interactions so that welding defects can be detected on real time monitoring and recording for an each workpiece ([Shao and Yan 2005](#)). In figure. 2.4 shows a process signals during laser welding. The reflected laser is the amount of the radiation of the laser source which is not absorbed by the material. Acoustic emission is divided into air-borne and structure-borne emission. There are originated from the stress waves induced by changes in the internal structure of a work piece. The metal vapour and the molten pool emit continuous radiation which spectrum varies with different laser application.

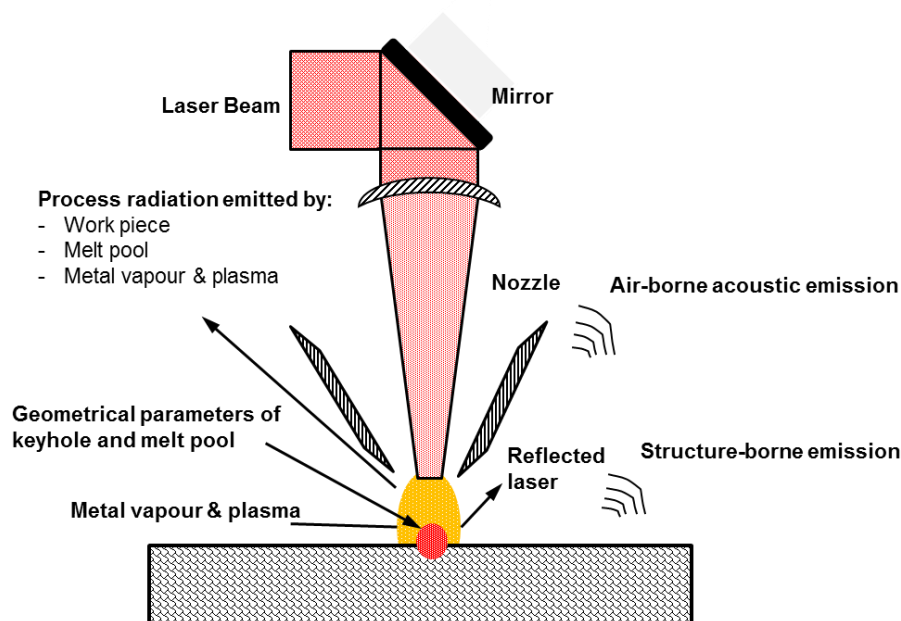


Figure 2.4 Process signals during laser welding(Duley, 1999)

2.4.1 Optical detector

For the optical detector, ultraviolet (UV) and infrared (IR) have mainly used to converted the flux density of the radiation emitted by the welding process into an electrical signal ([Shao and Yan 2005](#)). Figure. 2.4.1 is the typical setups using co-axial and off-axial arrangements.

Sibillano reported a real-time laser welding process using spectroscopy which is based on the acquisition of the optical spectra emitted from the laser generated plasma plume. He used a covariance mapping technique in order to measure the plasma electron temperature. From the plasma electron temperature, he added another chemical substance to each of a plasma plume and developed an algorithm that can analyze the defects ([Sibillano et al. 2009](#)).

Sergio suggested two kinds of monitoring approaches using spectroscopy. First approach is Photodiode-generated signal which is gathering radiation emitted by plasma mainly in the visible spectrum range. This is transforming into electrical signals and classifying according to their quality. Second approach is Electronic temperature-based method. It is the estimation of the electronic temperature and how to correlate it with weld quality is explained ([Sergio et al. 2010](#)).

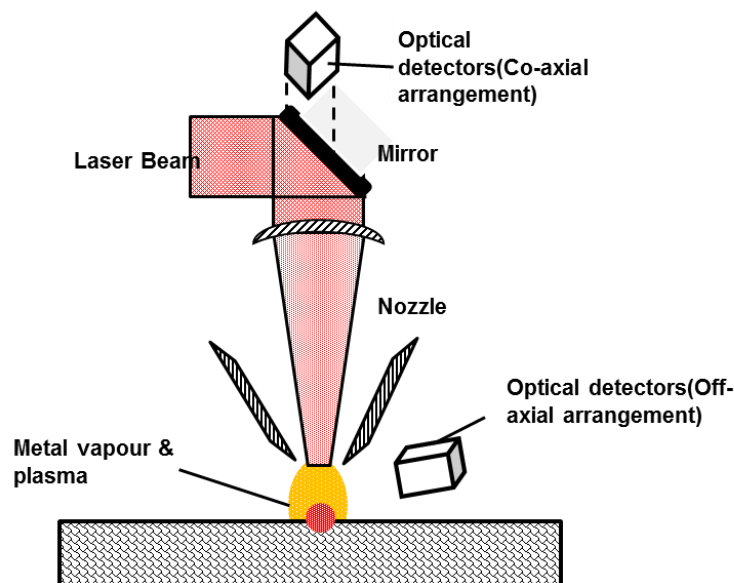


Figure 2.4.1 Typical setups for optical detectors using co-axial and off-axial arrangements.

Park reported a monitoring technique that can trace weld defects such as spatter and plasma using a photodiode sensor. This monitoring can detect the weld defects caused by changes in power and misalignment of focus ([Park et al. 2001](#)). Kang reported that weld quality can be detected in real time by plasma detector using plasma intensity. From the monitoring, they can figure out the correlation

between signal and weld quality ([Kang et al. 2006](#)). Jung reported that laser quality can be traced by chromatic aberration which can measure and analysis the thermal radiation from the molten pool so that it can measure the length of laser focus and size of molten pool, suggest an appropriate signal value, and control the welding state in real time ([Jung et al. 2000](#)).

2.4.2 Acoustic detector

One characteristic of laser welding is the acoustic emission which involves a sensor converting process sounds into electrical output to a measurable variable (Shao and Yan 2005). For the acoustic emission, air-borne emission and structure-borne emission are composed. The range of frequencies of air-borne emission is 20Hz to 20 kHz and those of structure-borne emission is 50kHz to 200kHz (Duley 1999; Shao and Yan 2005). Figure.2.4.2 describes typical experimental setups for acoustic emissions. One of the advantages of acoustic emission is that it can be firstly detected even subtle defects when defects are occurred. Kim measured both acoustic emission and plasma light emission in order to gather the information and define the correlations based on the different weld conditions (Kim 2002). Kim suggested the relationship between emission signals and weld defect for in-processing monitoring in order to approach the optimal lap welding condition using acoustic emission (Kim and Lee 2010).

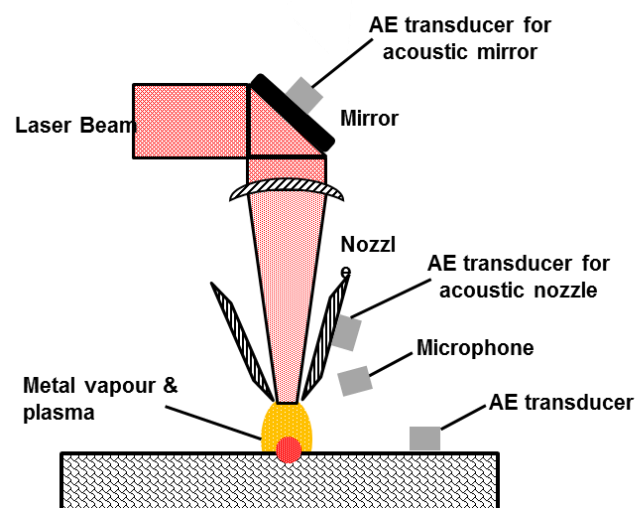


Figure 2.4.2 Typical setups for acoustic emissions

2.5 Part-to-part gap control

Recently, the enormous usage of thin steel sheets for automotive application for reducing car weight necessitates improved material strength as well as higher corrosion protection (Katundi, Tosun-Bayraktar et al. 2010). For these reasons, aluminum, zinc-coated, and magnesium alloys have been applied. However, all alloys need to keep a part-to-part gap because of sound weld parts. Not all the gaps can be guaranteed because all incoming materials cannot be flat shapes. Moreover, in galvanized steel sheets, when using galvanized steels, it is more difficult to keep the distance between gaps because of different temperature of melting and vaporizing point.

Many researches have studied in order to find out the optimal gap tolerance. In the literature reviews for gap controlling methods in galvanized steel sheets, there are three main sections: alternatives of creating gap, monitoring gap, and numerical optimizations.

2.5.1 Physical gap control method

Physical gap control method is mainly divided into five methods: De-gassing method, Zinc removal method, pulsed laser method, laser-hybrid method, and adding another element method. Table 2.5.1 shows the alternatives of creating gap including descriptions and authors.

De-gassing method

Chen (2009) reported a gap control method using CO₂ laser welding with galvanized steel sheets. He suggested that galvanized steel sheets with pre-drilled vent hole were carried out. In this concept, on the bottom part, pre-drilled holes were exploring and these holes allowed zinc vapor to escape freely (Chen et al. 2009). However, this concept cannot be realized because it has much time consuming and cost redundant to set up the pre-process.

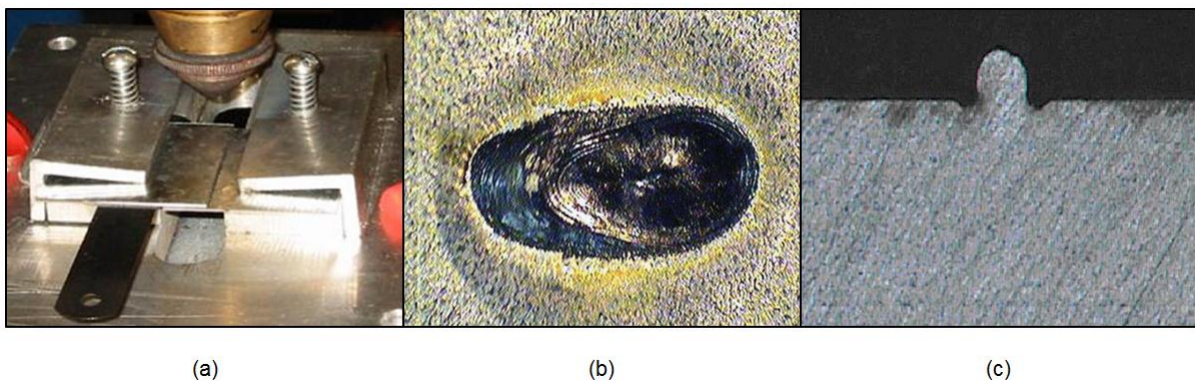


Figure 2.5.1 Three types of de-gassing methods: (a) pre-drilled hole, (b) dimpling, (c) humping effect (Chen et al. 2009; Gu 2010; Hongping and Boris 2011)

For the dimpling method (Gu 2010), it creates a small dimple (0.1mm to 0.2mm) to keep part-to-part gap in order to escape the zinc gases. This method also has some disadvantages: it needs pre-processing before welding and we cannot guarantee the exact range of dimple depended on varying thickness of materials. To minimize additional cost, humping effect was suggested for alternative degassing method (Hongping and Boris 2011). However, humping effect can only applied to the scanner welding because humping effect can be generated within faster time. In addition, the humping effect needs an angle around 50 degree which means every angle of beam should be changed depending on the variations of thickness of materials and material properties.

Removal of zinc layer

Another alternative part-to-part gap control is to remove the zinc-coated layer. Pennington (1987) suggested that the treated zone was replaced by nickel coating, which does not vaporize appreciably at the steel fusion temperature to reduce porosity and provide corrosion protection (Pennington 1987). But, disadvantage of this technique is the prohibitive additional processing cost or in other terms expensive in production environment.

Tian (2012) also suggested zinc removal method in order to prevent from the explosion or ejection of molten weld metal due to the pressure of zinc vapor (Tian and Zhang 2012). However, this method is also limited into the overlap welding and scanner weld-head.

Pulsed laser

Pulsed laser is the method for minimizing zinc-vaporization using high energy per pulse and short pulse duration. Heyden (1990) suggested that the lap welding without a gap can be possible when pulse repetition frequency and pulse energy are optimized (Heyden et al. 1990). Tzeng suggested that average peak power density is the most important factor when controlling in pulsed laser welding. In addition, by selecting proper parameters such as average peak power density, mean power, and welding speed. (Tzeng 1999; Tzeng 2000). However, the problems are that keyhole may not be occurred, and only high-power lasers can be achieved.

Laser hybrid

Recently, laser welding has become one of the most welding techniques in automotive industries. However, there are still problems about controlling gap between two dissimilar materials, especially series of zinc-coated steel sheet. For the lap welding, gap has to be extremely controlled between materials because of degassing of zinc vapor. For this reason, laser-arc hybrid welding has become distinguished. Laser-arc hybrid welding takes advantages of laser welding with arc welding(Defalco 2007).

Kim (2006) developed laser-arc welding method and its equipment for the galvanized steel (Kim 2006). In this patent, using laser-arc welding, arc discharge makes it vaporizing in order to prevent from the weld defects such as porosity, spatter, and blowhole. Ono (2002) also suggested a welding method preventing from the blowhole which the zinc tends to blow off the weld metal using laser-arc hybrid welding.

Additional elements

Mazumder (2002) invented a lap welding with copper sandwiching a foil sheet. The sandwiching method is to alloy with zinc to avoid violent evaporation between two materials, and a foil can absorb the vaporized zinc to form an alloy disposed between the two galvanized steel sheets. The thickness of filler material is between 0.0035 and 0.0045 inches (0.089mm and 0.114mm). Also, gas mixture was required which included Helium and Argon (Mazumder et al. 2002; Dasgupta and Mazumder 2006). Li suggested a new method in order to overcome the quality problems of gap control between zinc-coated steels. Diode laser welding and Nd:YAG laser welding were compared with an aluminum foil (25 μ m) between two zinc-coated steel sheets (1mm) (Li et al. 2007).

Kim suggested a method for a lap welding of magnesium alloy using Nd:YAG laser. Using stainless steel sheet (1.25mm), gap varied thickness 0.05 to 0.3mm. Optimal laser power is 2.5kW and welding speed is 55mm/s in order to reach a full penetration (Kim et al. 2011). Sun suggested the gap tolerance requirement by using wire feed welding. He used 2mm thickness of stainless steel with 3kW CO₂ laser welding and C-Mn steel wire. From the experiment, a desirable gap tolerance is about 1mm gap for 2mm thick butt welding (Sun and Kuo 1999).

Yang (2011) reported the weldability of galvanized steel sheets under the different shielding gas conditions. He proposed a side shielding gas which can restrain the laser induced plasma and plume. In the experiment, there were different conditions of shielding gas used: pure argon, helium, and the mixtures of argon and 25% and 10% CO₂, and mixture of argon and 2% O₂. The results showed that CO₂ or O₂ gas into the shielding gases or helium or the mixture of He and Ar instead of pure argon in order to be stable for galvanized steels were recommended. Another experiment with the active gases (O₂ and CO₂) showed that deeper penetration could be achieved when adding the active gas into the shielding gas as compared to the case of using pure argon. Moreover, single side shielding gas of pure Argon gas has sound lap joints with a gap-free configuration (Yang et al. 2011)

Wu (2008) investigated the relationship between welding penetration and width varying with laser power and welding speed. For preventing from the zinc vapour, Ar and N₂ were used as a side-blow protective shielding gas. The result showed that there was a little difference in maximal penetration, but there was no different in hardness, toughness of joint and Erichsen number of welding sample. Therefore, using Ar as protective gas showed better quality of weld of CO₂ laser

welding. In addition, the portion of zinc in weld seam can be controlled by applying to the side-blown protective gas as decreasing the cracks and holes at the HAZ (Wu et al. 2008).

Graham (1996) described the welding quality based on the different types of materials and welding methods. There are three types of materials (galvanized, galvanized, and electro-galvanized steels) and welding methods in order to control the gap (no gap, shim gap, groove-projection geometry, and edge welding). He suggested that good quality seam welds was the lap-welding with the galvanized steels and the permissible gap range was from 0.1mm to 0.2mm. In addition, in order to produce good quality of weld, the coating weight is important parameter at the interface of the lap welding (Graham et al. 1996).

Xie (2002) suggested a dual beam welding method which is one of the gap control welding methods. In the experiment, 6kW CO₂ laser beam was split into two equal-power beam and weld steel and aluminum plates. The results showed that improved weld surface conditions was presented, and spatter, weld hardness, and centerline cracking were reduced in steel welds. In addition, porosity, irregular beads, and spatter were decreased in aluminum plate. On the other hand, vapour plume fluctuation was still found, but the height and volume of the plume varied slightly (Xie 2002).

Kutsuna et al. 2002 developed Laser Roll Welding techniques which is useful for particularly joining of dissimilar materials. Laser roll welding decreases the formation of the brittle intermetallic compounds which formed at welding interface during laser welding process (Ozaki et al. 2010). In laser rolling welding we intentionally provided roller; roller generate roller pressure. Roller pressure facilitate adequate contact of two metal sheets (upper and lower) and also provide favorable conditions towards rapid heat transfer from a upper sheet to a lower sheet and these things are responsible for preventing the formation of brittle intermetallic compounds and lastly leads towards greater tensile strength and ductility. In case of laser welding of zinc coated steel, the roller pressure creates favorable conditions for escaping zinc oxide layer (which is also brittle in nature) from the welding interface (Katayama 2004).

There were various kinds of gap controlling methods, and many researches have made efforts to figure out how they control the gap of zinc coated materials. However, almost all methods have similar problems which make additional efforts or and waste of time or work process in negative aspects. In this study, we focus on the different directions of weld. One of the main reasons is that almost all incoming material in manufacturing industry are not always flat. This means that the shapes of incoming materials are concave or convex. That is why all part-to-part gaps are not stable even though gaps are fixed as 0.1mm-0.3mm. Furthermore, it is so hard to be in research field because convex or concave shapes of materials are randomly income.

In this study, we simplify the complex models of materials into the linear models (Figure 2.5.2). Firstly, we assumed that all the incoming materials are flat and stable part-to-part gaps are existed. In addition, we deliberately make artificial gap which is from 0.1mm to 0.3mm only for the one side. From the experiment, we figure out whether the direction of weld can affect the welding quality such as shear strength and discuss the relationship between directions of weld.

Table 2.5.1 The methods of alternatives creating gap

Methods	Description	Related work
De-gassing methods	- Pre-drilled hole	Chen et al. 2009;
	- Dimpling	Shulkin 2011; Gu, 2010;
	- Humping effects	Hongping and Boris 2011;
Removal of zinc layer	- Removal of zinc coating and replace it with an element with a higher boiling point like nickel	Pennington 1987; Zhang and Tian 2012
Pulsed laser	- Pulsed lasers that have high energy per pulse and short pulse duration to minimize vaporization	Tzeng 1999; Tzeng 2000
Hybrid	- YAG laser-arc hybrid	Ono et al. 2002;
	- CO2 laser-TIG arc hybrid	Kim et al. 2006
Additional elements		Pecas et al. 1995;
		Li et al. 2007;
		Lee 2009;
		Mei et al. 2009;
		Chen et al. 2011;
	- Using aluminum foil between zinc-coated steel sheets	Yang et al. 2011;
	- Shielding gas disrupting plasma formation	Mazumder et al. 2002;
	- Dual beam welding	Dasgupta and Mazumder 2006;
	- Laser roll welding	Wu et al. 2008;
		Graham et al. 1996;
		Xie 2002;
		Ozaki et al. 2010;
		Katayama 2004

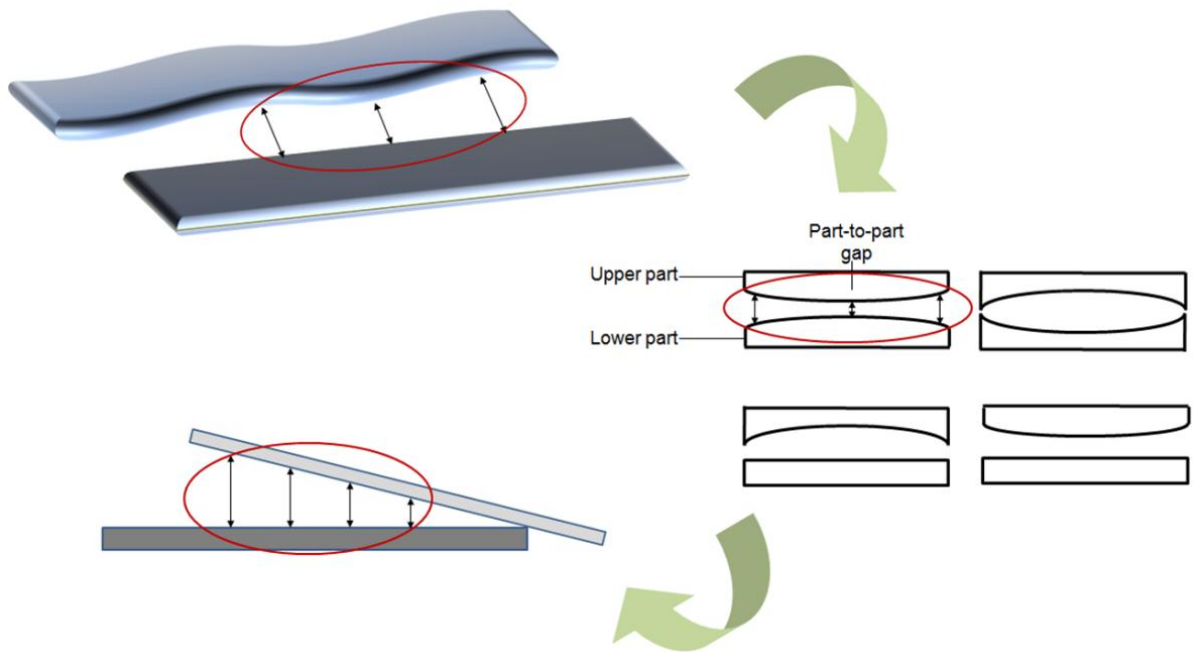


Figure 2.5.2 A schematic drawing of simplifying the concave model into the linear model

III. Experimental design

3.1 Laser welding system

Fiber laser welding

In order to obtain good beam quality in a high-power laser, cooling of the medium is necessary. For this reason, a fiber laser was developed in order to shorten the rod diameter and lengthen the rod size. A fiber laser consists of pump diode laser, a ytterbium active fiber, and fiber Bragg grating, as shown in Figure. 3.2.1(Han 2010). Two important characteristics of a fiber laser are its strength against external shock and the fact that it is not necessary to arrange the optical system. A fiber laser whose wavelength is 1.03 μm offers the preferred wavelength range for metal processing owing to the high material absorption it facilitates (IPG Photonics 2010). One characteristic of fiber laser is to be strong against external shock and no necessary to arrange the optical system. A fiber laser whose wavelength is 1.03 μm offers the preferred wavelength range for metal processing due to high material absorption(IPG Photonics 2010). In addition, the single emitter diode of a fiber laser is not affected by heat effects, and provides stable energy consumption. Moreover, because of its active cooling water system, there is no need to use deionized water, so a uniform temperature can be maintained. Lastly, it provides fast on/off operation, so there is no waiting time.

In this study, an IPG YLR-2000-AC ytterbium-doped fiber laser source was used. The maximum laser power is 2 kW, and two channels (200 μm and 600 μm fiber cables) are available. Table 3.1.1 lists the specifications of the fiber laser source, and Table 3.1.2 lists, the specifications of the laser welding system at UNIST. The laser welding system, which was adapted by SIS Corporation, is composed of a CNC machine that has X, Y, and Z axes. In addition, it has three kinds of focus lenses (160 mm, 300 mm, and 500 mm), each of which has focal lengths of 139 mm, 273 mm, and 465 mm, respectively. Figure 3.1.3 shows the laser welding system at UNIST. For this experiment, a 200 μm fiber cable and a 160 mm focus lens were utilized. The spot size at UNIST is 200 μm , and the equation is as shown below Figure 3.1.2.

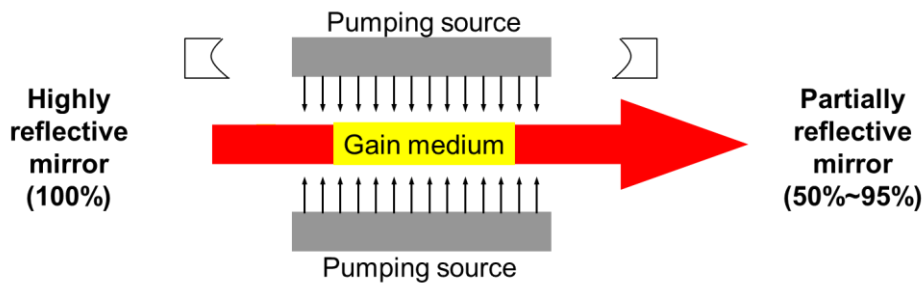


Figure 3.1.1 Principle of a laser (Sungwoo Hightech., Ltd)

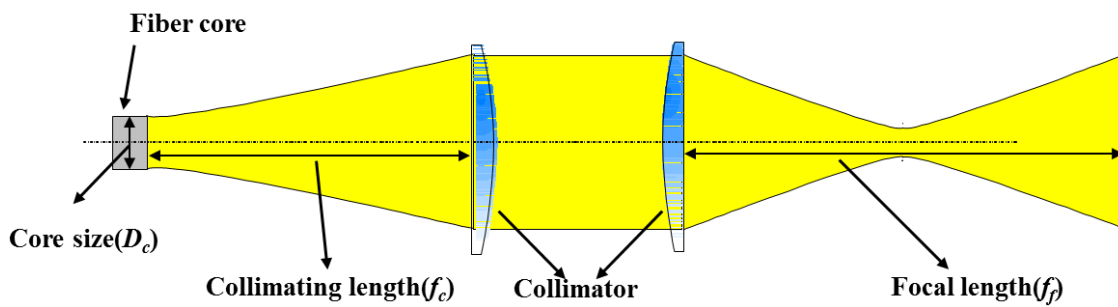


Figure 3.1.2 Optical dimensions of core diameter (adopted from Mazumder, 2010)

An IPG fiber lens has a collimator lens that adjusts the laser power to a suitable degree. An optical dimension for the fiber diameter has a fiber core and a collimator. In order to determine the spot size of a fiber laser, the following equation is used:

$$\text{Spot size (diameter)} = \frac{f_f}{f_c} \times D_c \text{ [}\mu\text{m]}$$

If we apply this equation to the example of a focal length of 160 mm, a collimating length of 160 mm, and a core size of the fiber of 200 μm , we obtain a spot size of 200 μm .

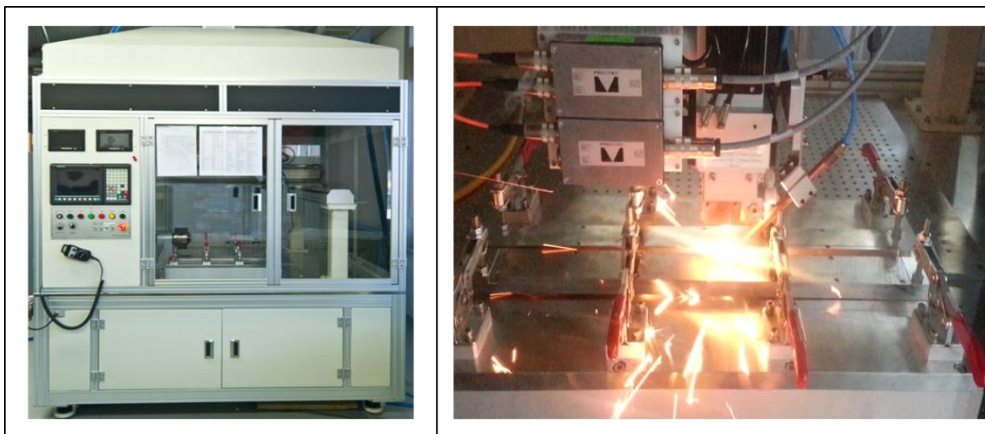


Figure 3.1.3 Fiber laser welding system (left) and welding with clamping (right)

Table 3.1.1 A specification of fiber laser welding

Product	IPG YLR-2000-AC
Maximum Laser power	2 kW
Laser mode	TEM01
Focus length	168 mm
Operation mode	CW
Switching ON/OFF time	80 micro-sec
Emission wavelength	1070 nm
Output power Instability	2.0%
BPP*(1/e ²) at the output of Fiber	2.0mm*mrad
Maximum Laser power	2 kW
Laser mode	TEM01

Table 3.1.2 A specification of laser welding system at UNIST

Fiber diameter	200μm, 600μm
Focus lens	160mm, 300mm, 500mm
Focal length	139mm, 273mm, 465mm
Stroke of X, Y, and Z axis	600mm, 800mm, 400mm
Maximum speed of X, Y, Z axis	30000mm/min, 30000mm/min, 12000mm/min

3.2 Experimental material

The experimental materials consisted of 1.8-mm-thick (SGARC440) and 1.4-mm-thick (SGAFC590DP) galvanized steel sheets. Each material had a different coating weight. The 1.8-mm-thick hot-dipped galvanized steel sheet had 43.5 g/m² of top plate and 45.5 g/m² of bottom plate, whereas the 1.4-mm-thick dual-phase steel sheet had 41.3 g/m² of top plate and 45.4 g/m² of bottom plate. Table 3.2.1 lists the chemical compositions of SGARC440 and SGAFC590DP. Both materials have been applied to Hyundai Motor Company's Verna automobile (Figure 3.2.1). In addition, the two materials were lap-welded, based on a thickness of 1.4 mm for the upper part of the material and 1.8 mm for the lower part. The width of each specimen was set at 30 mm, and the length of each specimen at 100 mm. The material used is the same as that used in a side member having an inner part (1.8 mm) and an outer part (1.4 mm).



Figure 3.2.1 Side member of a vehicle (SungWoo Hi-tech)

Table 3.2.1 Chemical composition of galvanized steel sheets

Material	C (%)	Si (%)	Mn (%)	P (%)	S (%)
SGARC440 (1.8 mm thickness)	0.12	0.5	1.01	0.021	0.004
SGAFC590DP (1.4 mm thickness)	0.09	0.26	1.79	0.03	0.003

3.3 Part-to-part gap

An artificial gap needed to be created in order to degas the zinc vapor. In the experiment, a shim gauge was used, in varying thicknesses ranging from 0.01 mm to 1 mm (Figure 3.2.2). The shim gauge was set up for 2 modes of usage, parallel and one-sided. Figure 3.2.3 shows a 3D model of the lap welding schematic of fiber laser welding.

Before doing experiments, a variety of ranges for part-to-part gap was considered. Pilot test for ranges of par-to-part gap, the range of 0.0 mm to 0.5 mm gap was carried out. When a permissible range of gap was more than 0.3 mm, two sheets were not jointed because the gap was so large that melted pool could not move to the lower part of sheet. Even if the two specimens were jointed, the only starting point was jointed because of high input energy of that point.

In addition, as mentioned that the thickness of galvanized steel sheets are 1.4 mm of thick and 1.8 mm of thick, setting the welding speed parameter is important. In the experiment, 2100 mm/min of welding speed was set as a fixed parameter. During the pilot test, we changed the welding speed 1200 mm/min to 3600 mm/min. Within the capability of our machine, 2100 mm/min of welding speed was proper. In the section of 1200 mm/min to 1500 mm/min, which is the interval of low speed, there are many spatter, porosity, and blow holes. In other word, from the 2700 mm/min to 3600 mm/min, which the welding speed is too high, full penetration was not achieved from the welding speed of 0.2mm/min. Therefore, we decided that the optimal welding speed parameter was set as 2100 mm/min in order to joint two steel sheets.



Figure 3.2.2 Shim gauge

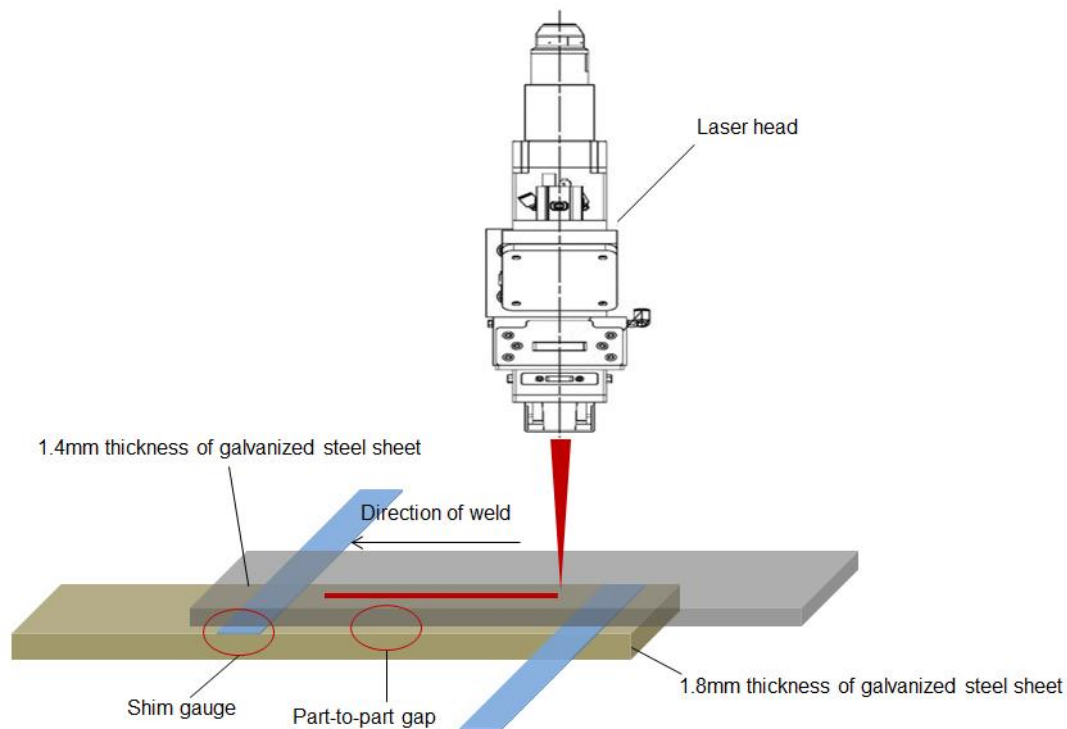


Figure 3.2.3 A schematic drawing of lap welding of fiber laser welding

3.4 Direction of welding

As we mentioned earlier, the purpose of this research is to ascertain the effects of a part-to-part gap and the direction of welding. This is why three types of welding are of interest. The first type is lap welding in a direction of ascendance. The second type involves a uniform gap. The third type is also lap welding, but in a direction of descendance (Figure 3.3.1). In the experiment, we assumed that all specimens are flat so that the results of tensile test have a normal distribution, which means there is no noise in the experiment.

When welding of side member, stitch, 'c' type, 's' type, and continuous welding have been tested. But, in the research field, only short ranges of welding were examined, which range were around 15 mm to 30 mm. This range cannot confirm the quality of welding in reality. In addition, the length of stitch welding for side member was applied as 40 mm in the automotive industry. Therefore 40 mm of welding length was set as length of weld bead. In the experiment, 40 mm length of weld bead was considered as the limits of specimen. Total width of specimen is 130 mm. Except for lap parts which is 30 mm x 30 mm of square for the tensile strength test, the maximum length of weld bead was 40 mm. For the future research, the variation of weld bead related to the weld quality will be progressed.

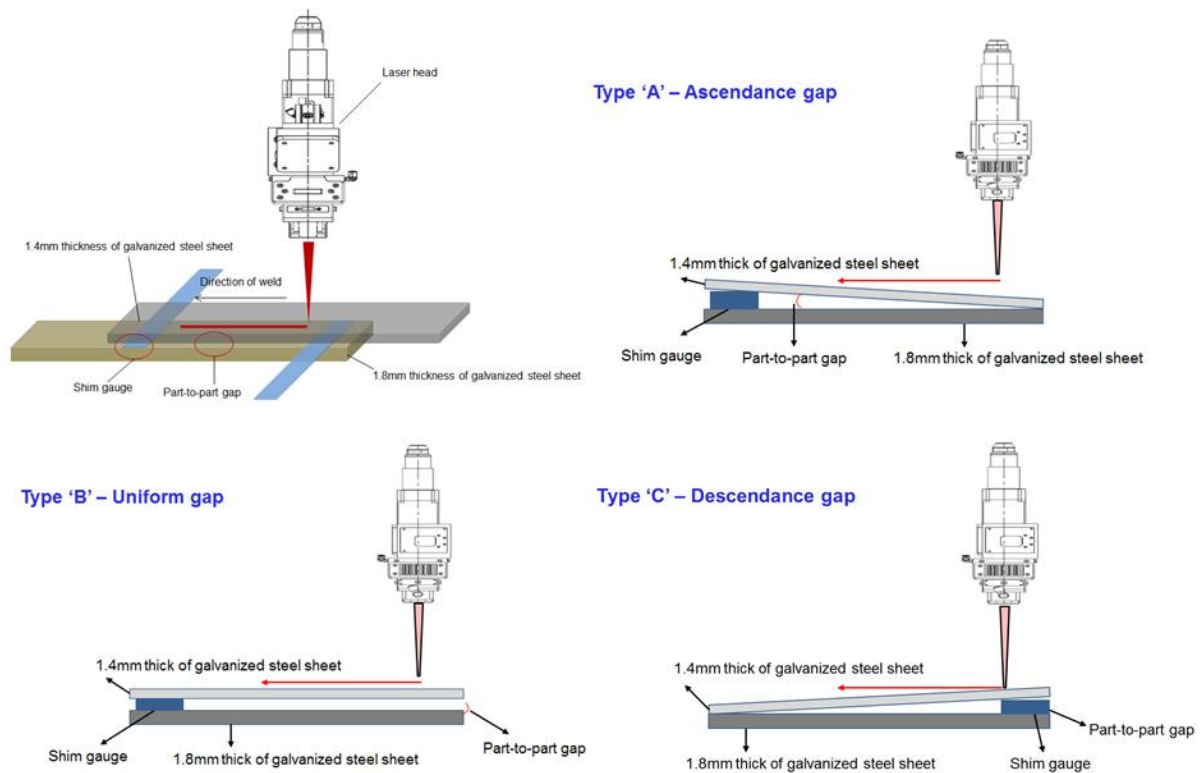


Figure 3.3.1 Schematic drawings of three types of laser methods

3.5 Laser welding parameters

The welding speed was fixed at 2100 mm/min, using laser powers of 1400 W, 1700 W, and 2000 W. Moreover, a 3³ factorial design with 3 replications was carried out randomly in order to determine a reasonable p-value, using an ANOVA table.

In Table 3.5.1, which shows the experimental design of the laser welding, “LP” denotes laser power, “G” denotes the part-to-part gap, and “D” denotes the direction of weld. All experiments were carried out randomly. Each individual process parameter was selected based upon a number of experiments, and each parameter had its own coded value.

Table 3.5.1 Experimental design of laser welding

Level	Laser power (LP) (kW)	Part-to-part gap (G) (mm)	Weld of direction (D)	Coded value
1	1400	0.1	Ascendance	-1
2	1700	0.2	Uniform gap	0
3	2000	0.3	Descendance	1

In addition, shear tensile strength was applied in our measurement of weld quality, because it is a very important factor in recognizing the relationship between a laser's input parameters and output parameters. The experiment was carried out in a total of 27 trials with three replications which were 81 experiments in total, and the steepest ascent method was performed in additional experiments in order to measure the maximum shear tensile strength.

In this study, we assumed that the shear tensile strength for the direction of ascendance would be higher than it would be for the direction of descendance, because the heat input into the material would play a role in pressing upon materials when the laser performs welding with no part-to-part gap. On the other hand, descending welding would produce weak shear tensile strength because the gap would be too wide to weld if the laser is welded from the gap. Moreover, a keyhole would not be generated and full penetration would not be achieved. Figure 3.3.2 shows the hypothetical design of welded parts based on the different welding directions. In the hypothesis, the width of the gap would reduce when welding in a direction of ascendance, as shown in Type (a) of Figure 3.3.2, and full penetration would be achieved. In the direction of descendance, however, full penetration of the gap would be difficult in a 0.2-mm gap and 0.3-mm gap because the width of the gap would be so great that laser welding would not be able to penetrate the entire material.

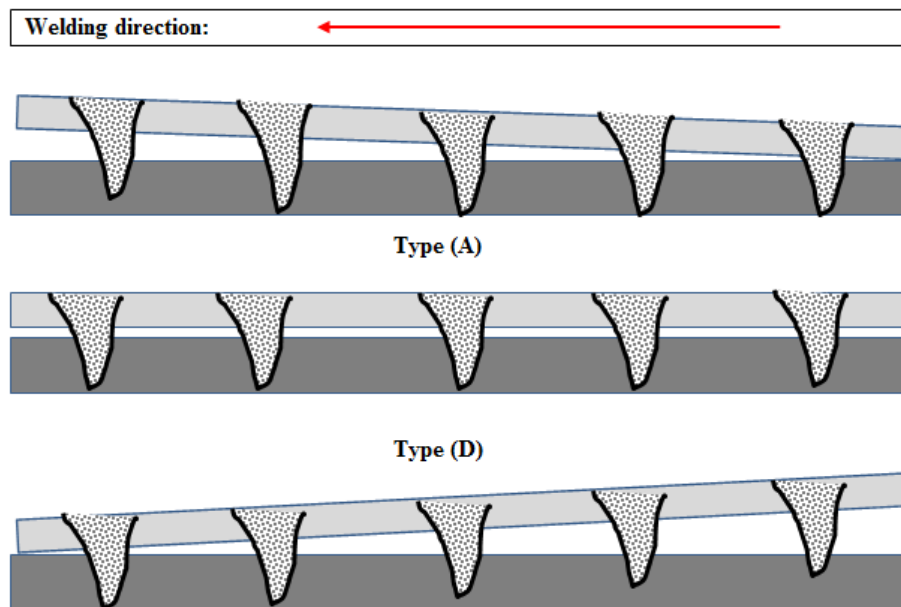


Figure 3.5.2 Hypothetical design of welded part based on the different types of welding

IV. Analysis of experiment

In this research, we sought to ascertain which factors can produce significant effects on the quality of laser welds. Therefore, we carried out an analysis of variance (ANOVA) in order to verify whether or not the experiments indicated important factors. In addition, for each direction of welding, such as ascendance gap and descendance gap, we determined the maximum tensile shear value using the steepest ascent method, so that we approached the new area to reach the maximum strength.

4.1 Analysis of Variance

ANOVA is used to test the equality of several means in order to verify whether or not an experiment has produced significant results (Montgomery 2008). As mentioned in Chapter 3, 3 factors and 3 levels of factorial design were conducted with three replications. Table 4.1.1 shows the design matrix with the three replications used in the experiment. Further, Table 4.1.2 shows the results of the ANOVA table for the 3 replications.

Table 4.1.1 Design matrix with code process parameter and response parameter

No.	<i>LP</i>	<i>G</i>	<i>D</i>	<i>Laser Power (W)</i>	<i>Gap (mm)</i>	<i>Direction of weld</i>	<i>Replica 1</i>	<i>Replica 2</i>	<i>Replica 3</i>
1	0	-1	-1	1700	0.1	Ascendance	228.1240	196.8951	177.5496
2	0	-1	1	1700	0.1	Descendance	92.8845	116.9284	101.5592
3	-1	-1	-1	1400	0.1	Ascendance	102.6944	100.2627	119.5499
4	0	1	1	1700	0.3	Descendance	229.9772	229.9772	222.4619
5	0	-1	0	1700	0.1	Uniform	102.5016	212.8497	76.8476
6	0	1	0	1700	0.3	Uniform	219.8497	244.9348	227.7001
7	1	1	0	2000	0.3	Uniform	269.0149	263.1319	232.9825
8	1	1	1	2000	0.3	Descendance	230.4439	228.8583	238.2257
9	-1	1	0	1400	0.3	Uniform	163.6654	225.6113	204.599
10	1	0	-1	2000	0.2	Ascendance	240.7452	228.8207	237.2453
11	-1	0	-1	1400	0.2	Ascendance	215.9365	122.1903	202.7458
12	0	1	-1	1700	0.3	Ascendance	163.5098	226.8219	240.0204
13	-1	-1	0	1400	0.1	Uniform	58.7752	159.9925	65.7663
14	0	0	-1	1700	0.2	Ascendance	159.9925	226.0880	227.0853
15	-1	1	1	1400	0.3	Descendance	158.4136	95.3283	96.5552
16	0	0	1	1700	0.2	Descendance	229.0039	120.9113	188.1045
17	-1	0	0	1400	0.2	Uniform	199.9851	165.9782	166.0172
18	-1	1	-1	1400	0.3	Ascendance	168.9943	219.7883	176.3852

CHAPTER 4

19	1	0	1	2000	0.2	Descendance	229.0039	170.7031	172.0524
20	0	0	0	1700	0.2	Uniform	224.1691	224.3528	228.2054
21	-1	-1	1	1400	0.1	Descendance	104.1158	112.1213	98.396
22	1	-1	0	2000	0.1	Uniform	250.4549	238.1551	230.7759
23	1	1	-1	2000	0.3	Ascendance	246.0974	237.1049	237.0161
24	1	-1	-1	2000	0.1	Ascendance	204.4080	184.6933	243.7357
25	1	0	0	2000	0.2	Uniform	240.7462	227.3549	226.8726
26	-1	0	1	1400	0.2	Descendance	116.2084	87.72321	90.2105
27	1	-1	1	2000	0.1	Descendance	251.8514	179.2699	148.8539

Table 4.1.2 ANOVA table for 3 replication

	<i>SS</i>	<i>DOF</i>	<i>MS</i>	<i>F₀</i>	<i>P-value</i>
<i>LP</i>	97881.1	2	40940.5	43.81	0.00001
<i>G</i>	42060.5	2	21030.2	18.4	0.00001
<i>D</i>	<u>30642.9</u>	<u>2</u>	<u>15321.5</u>	<u>13.4</u>	<u>0.00001</u>
<i>LP*G</i>	9450.4	4	2362.6	2.07	0.096
<i>LP*D</i>	3275.3	4	818.8	0.72	0.584
<i>G*D</i>	4667.5	4	1166.9	1.02	0.4037
Error	70881.4	62	1143.2		
Total	258859	80			

Block effect

Before the analysis of results, we need to check whether the noises or errors disrupting could cause the results or not. Therefore, the experimental conditions should be ensured that the treatments are equally effective using blocking design. In this result, three blocks can be separated. Table 4.1.3 shows the experiment in three blocks.

Table 4.1.3 Experiment in Three Blocks

	Block 1	Block 2	Block 3
	228.1240	196.8951	177.5496
	92.8845	116.9284	101.5592
	102.6944	100.2627	119.5499
	229.9772	229.9772	222.4619
	102.5016	212.8497	76.8476
	219.8497	244.9348	227.7001
	269.0149	263.1319	232.9825
	230.4439	228.8583	238.2257
	163.6654	225.6113	204.599
	240.7452	228.8207	237.2453
	215.9365	122.1903	202.7458
	163.5098	226.8219	240.0204
	58.7752	159.9925	65.7663
	159.9925	226.0880	227.0853
	158.4136	95.3283	96.5552
	229.0039	120.9113	188.1045
	199.9851	165.9782	166.0172
	168.9943	219.7883	176.3852
	229.0039	170.7031	172.0524
	224.1691	224.3528	228.2054
	104.1158	112.1213	98.396
	250.4549	238.1551	230.7759
	246.0974	237.1049	237.0161
	204.4080	184.6933	243.7357
	240.7462	227.3549	226.8726
	116.2084	87.72321	90.2105
	251.8514	179.2699	148.8539
Block total	5101.5668	5046.84741	4877.5192

 SS_{Block}

$$= \sum_{i=1}^3 \frac{B_i^2}{27} - \frac{y^2 \dots}{27}$$

$$= \frac{(5101.57)^2 + (5046.85)^2 + (4877.52.57)^2}{27} - \frac{(15026)^2}{81}$$

$$= 1010.66$$

Table 4.1.4 ANOVA table for 3 replication in three blocks

	<i>SS</i>	<i>DOF</i>	<i>MS</i>	<i>F₀</i>	<i>P-value</i>
<i>Block</i>	1016.7	2	505.3		
<i>LP</i>	97881.1	2	40940.5	36.33	0.00001
<i>G</i>	42060.5	2	21030.2	18.7	0.00001
<i>D</i>	30642.9	2	15321.5	13.6	0.00001
<i>LP*G</i>	9450.4	4	2362.6	2.1	0.096
<i>LP*D</i>	3275.3	4	818.8	0.72	0.58
<i>G*D</i>	4667.5	4	1166.9	1.03	0.403
Error	69864.7	62	1126.9		
Total	258859	80			

When applying block effect from the Table 4.1.2, there are two degrees of freedom among the three blocks. Table 4.1.4 indicates that the conclusions from this analysis, had the design been run in blocks, are identical to those in Table 4.1.2 and that the block effect is relatively small. That is, there are only few noises and errors remained.

4.2 Comparison between two different types of directions

When we found that direction of weld is an important factor as a quality of weld, we also have to figure out how the direction of weld can affect the maximum shear strength. To compare two different value of strength, t-Test was carried out, and approached to the maximum shear strength in advanced area using steepest ascent method.

4.2.1 t-Test

t-Test is to verify whether the means of two groups are statistically different from each other. In this research, mean values were compared with $\alpha = 0.05$, based on the direction of Ascendance and direction of Descendance. The statistical hypothesis was stated formally as

μ_1 : Direction of ascendance,

μ_2 : Direction of descendance

$$H_0: \mu_1 = \mu_2$$

$$H_1: \mu_1 < \mu_2$$

Within $\alpha = 0.05$, the p-value is 0.024, which means that this result is significant and we can accept the H_0 . Therefore, we concluded that the average of the direction of ascendance is higher than those of descendance. Table 4.2.1 shows the result of t-Test for two different directions of welding.

Table 4.2.1 The results of t-Test from the two different directions of welding

	Direction of ascendance	Direction of descendance
Sample size	9	9
Mean	213.35	162.96
90% confidence interval	(187.8, 238.9)	(128.13, 197.79)
Standard deviation	41.219	56.196
Difference between two means	50.392	
90% confidence interval	(9.4758, 91.308)	

4.2.2 Steepest ascent method

As mentioned before, we need to find the maximum shear strength based on each an different direction of welding. The steepest ascent method is a procedure moving to the maximum point while input parameters are varying. Figure 4.2.1 is the schematic of steepest ascent method.

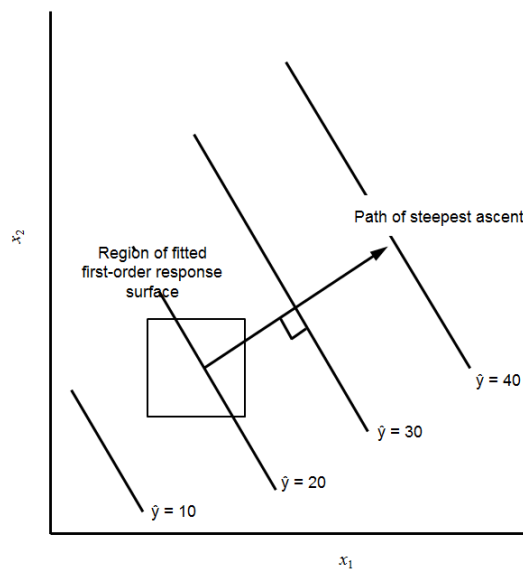


Figure 4.2.1 A schematic of First-order response surface and path of steepest ascent (Montgomery 2008)

From the experimental design, laser power, part-to-part gap, and direction of weld were the factors. However, when it comes to the maximum shear strength based on the direction, another fixed factor is considered as a direction. In addition, collected data is a 2^2 factorial augmented by five center points because replicates at the center points are used to estimate the experimental error and to allow for checking the adequacy of the first-order model (Montgomery 2008).

Table 4.2.2 shows the process data for fitting the first-order model of direction of ascendance. In this case, we concluded that the average shear tensile strength of Ascendance is higher than those of Descendance. So, we considered only ascendance factor because our goal is to find out the maximum shear tensile strength. A first-order model is fit to the data by least squares and the equation of the first-order model is shown below:

$$\hat{y} (\text{Ascendance}) = 213.352852 + 46.204158 x_1 + 12.528933 x_2$$

Table 4.2.2 Process data for fitting the first-order model

Coded variables		Natural variables		Responses
x_1	x_2	<i>LP</i>	<i>Gap</i>	<i>Shear tensile strength (y)</i>
<i>Ascendance</i>				
-1	-1	1400	0.1	119.5499
-1	1	1400	0.3	176.3852
1	-1	2000	0.1	243.7357
1	1	2000	0.3	237.0161
0	0	1700	0.2	227.0853
0	0	1700	0.2	215.9365
0	0	1700	0.2	218.3661
0	0	1700	0.2	250.7567
0	0	1700	0.2	231.3442

Before approaching the path of steepest ascent, we should investigate the adequacy of the first-order model. (Montgomery 2008) suggests the 3 steps before exploring the path of steepest ascent shown below:

1. To obtain an estimate of error.
2. To check for interactions in the model.
3. To check for quadratic effect (curvature).

Table 4.2.3 shows the analysis of variance for the first-order model based on the directions of both Ascendance and Descendance. From those tables, interaction and pure quadratic (curvature) are negligible. Therefore, there is no indication of the interaction and pure quadratic effect.

Table 4.2.3 Analysis of variance for the first-order model (Ascendance)

<i>Source</i>	<i>SS</i>	<i>DOF</i>	<i>MS</i>	<i>F₀</i>	<i>P-value</i>
Model (β_1, β_2)	10193	2	5096.4	6.9111	0.0277
Residual	4424.6	6			
(Interaction)	1009.8	1	1009.8	5.2745	0.0832
(Pure quadratic)	2649	1	2649	13.8365	0.0205
(Pure error)	765.7955	4	191.4489		
Total	14617	8			

To move away from the center point ($x_1 = 0, x_2 = 0$) along the path of steepest ascent, we would choose a step size in one of the process (input) parameters, Δx_1 . We can select the parameter that we have known. The equation for Δx_i is followed by,

$$\Delta x_i = \frac{\hat{\beta}_i}{\hat{\beta}_j / \Delta x_j}$$

From the equation, we can find Δx_i of depending on the two directions of the Ascendance and Descendance. Table 4.2.4 is the steepest ascent experiment for the direction of ascendance.

Table 4.2.4 Steepest ascent experiment for the direction of Ascendance

Steps	x_1	x_2	<i>LP(W)</i>	<i>Gap(mm)</i>	Shear strength (MPa)
Origin	0	0	1700	0.2	
Δ	1	0.271	50	0.02	
Origin + Δ	1	0.271	1750	0.22	224.4709
Origin + 2Δ	2	0.542	1800	0.24	234.26556
Origin + 3Δ	3	0.813	1850	0.26	233.63689
Origin + 4Δ	4	1.084	1900	0.28	235.66922
Origin + 5Δ	5	1.355	1950	0.3	242.66525
Origin + 6Δ	6	1.626	2000	0.32	247.58665
Origin + 7Δ	7	1.897	2050	0.34	243.83757

When it comes to the plot, Figure 4.2.2 shows each step along the path of steepest ascent. The direction of welding performed the maximum shear strength. For the direction of Ascendance, increases in response are observed through the 6 step. However, after 6 step, response is decreased. In this situation, further experiments could not be proceeded because a capacity of laser power in UNIST is up to 2kW. For the direction of descendance, increases in response are observed through the 4 step. After then, all the responses tend to be decreased. Therefore, the maximum shear strength of Ascendance is 247.59 MPa when laser power is 2000W, Welding speed is 2100mm/min, and part-to-part gap is 0.32mm.

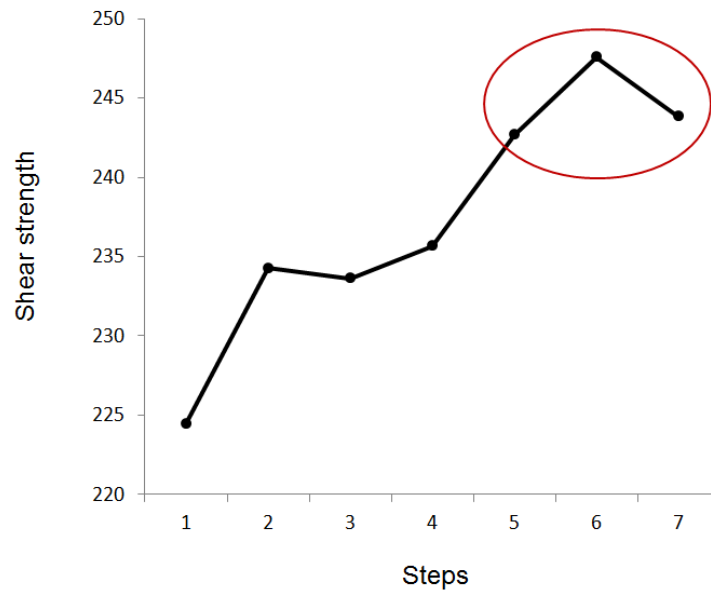


Figure 4.2.2 Shear strength versus steps along the path of steepest ascent for direction of Ascendance (Welding speed: 2100 mm/min)

Table 4.2.5 Process data for second first-order model

Coded variables		Natural variables		Responses
x_1	x_2	LP	Gap	<i>Shear tensile strength</i> (y)
<i>Ascendance</i>				
-1	-1	1950	0.3	242.6653
-1	1	1950	0.34	252.2187
1	-1	2050	0.3	244.771
1	1	2050	0.34	243.8376
0	0	2000	0.32	255.5581
0	0	2000	0.32	256.117
0	0	2000	0.32	253.2866
0	0	2000	0.32	252.8504
0	0	2000	0.32	253.1996

A new first-order model is fit around the point ($LP = 2000$, $Gap = 0.32$). The region of exploration for LP is [1950, 2050], and it is [0.3, 0.34] for Gap. Thus, the coded variables are,

$$x_1 = \frac{LP-2000}{5} \text{ and } x_2 = \frac{Gap-0.32}{5}$$

Once again, a 22 design with five center point is used. The experimental design is shown in Table 4.2.5. And the new first-order model fit to the coded variables in Table 4.2.5 is,

$$\hat{y} \text{ (ascendance)} = 250.500461 - 1.568857 x_1 + 2.155018 x_2$$

The analysis of variance for this model is shown in Table 4.2.6. The interaction and pure quadratic checks imply that the first-order model is not an adequate approximation. This curvature in the true surface may indicate that we are near the optimum. At this point, additional analysis must be done to locate the optimum more precisely.

Table 4.2.6 Analysis of variance for the first-order model (Ascendance)

<i>Source</i>	<i>SS</i>	<i>DOF</i>	<i>MS</i>	<i>F₀</i>	<i>P-value</i>
Model (β_1, β_2)	58.537	2	29.268	0.9202	0.4482
Residual	190.837	6			
(Interaction)	27.4936	1	27.4936	11.9856	0.0258
(Pure quadratic)	154.168	1	154.168	67.2082	<u>0.0012</u>
(Pure error)	9.175	4	2.2939		
Total	249.3741	8			

4.3 Comparison of the shear tensile strength with directions of Ascendance and Descendance

As noted in the previous sub-chapter, we learned from the ANOVA results that the direction of the weld can have a considerable effect upon its quality (shear tensile strength), and that by applying a t-Test, a difference was found between the ascending and direction of descendance. We also determined the maximum shear tensile strength of the direction of ascendance using the steepest ascent method. In this chapter, a comparison between the shear tensile strength achieved by two different welding directions and weld microstructures will be described, as corroboration of the main intent of this thesis.

Before making a comparison between the two different welding directions, we created a number of graphs related to the maximum shear tensile strength. The results were obtained from the average maximum shear tensile strength with 3 replications. Figure 4.3.1 shows the different patterns produced by the different types of welding direction. These graphs were created for the cases of a uniform gap, and ascending and direction of descendance. As shown in Figure 4.3.1, the shear tensile strength is strongly related to the laser power and the gap. With 1400 W of laser power, (a) and (b) display the same patterns on the graph, while the strength of (c) expresses a low value. With 1700 W of laser power, (b) shows an increase along the increasing gap, while (a) and (c) show a rapid graph based on the increase in the gap. These results show that the direction of ascendance produces a linearly stable weld bead as well as a weld quality that is superior to that in the other two directions.

We then concluded that the shear tensile strength is greater for the direction of ascendance than for the direction of descendance. In order to verify that conclusion, a t-Test was carried out, because there were some variations between these two directions.

Before performing the t-Test, the maximum parameters (LP: 2000 W, WS: 2100 mm/min, and G: 0.32 mm) were applied based on the two different weld directions. Table 5.1.1 and Table 5.1.2 present the results for the respective shear tensile strengths. The maximum shear tensile strength for the direction of ascendance was 260.4549 MPa, whereas that for the direction of descendance was 254.9782 MPa.

At the same time, the average shear tensile strength for the direction of ascendance was 255.8704MPa, and that for the direction of descendance was 245.5632 MPa. To verify that there was a difference between the two different weld directions, a t-Test was carried out.

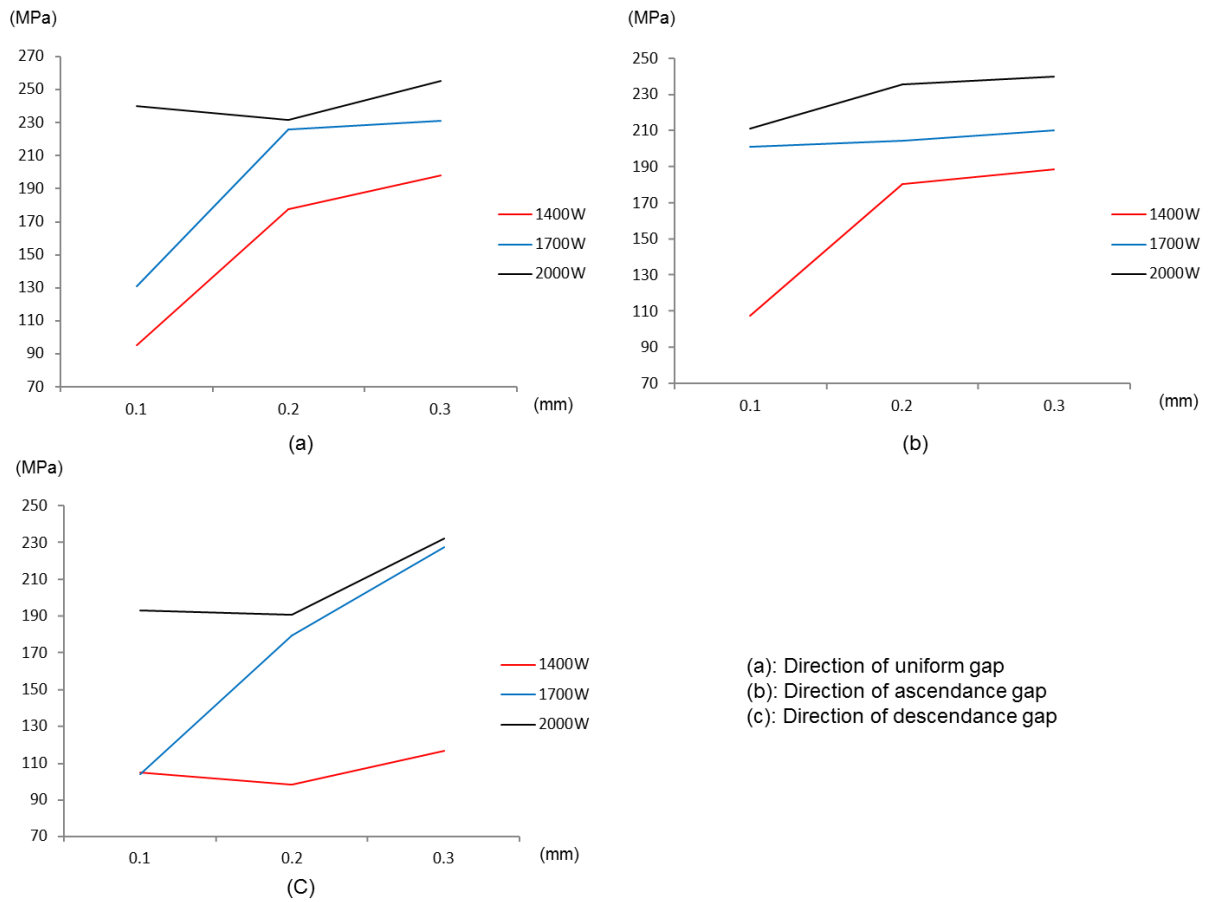


Figure 4.3.1 Different patterns of graphs for different types of weld direction

Table 4.3.1 Maximum shear tensile strength with 9 replications (Ascendance)

Run	LP	WS	G	D	Shear tensile strength
1	2000	2100	0.32	Ascendance	255.5581
2	2000	2100	0.32	Ascendance	256.117
3	2000	2100	0.32	Ascendance	253.2866
4	2000	2100	0.32	Ascendance	267.8478
5	2000	2100	0.32	Ascendance	269.4549
6	2000	2100	0.32	Ascendance	246.3622
7	2000	2100	0.32	Ascendance	252.8504
8	2000	2100	0.32	Ascendance	253.1996
9	2000	2100	0.32	Ascendance	248.1572

Table 4.3.2 Maximum shear tensile strength with 9 replications (Descendance)

Run	LP	WS	G	D	Shear tensile strength
1	2000	2100	0.32	Descendance	233.3469
2	2000	2100	0.32	Descendance	243.963
3	2000	2100	0.32	Descendance	240.3396
4	2000	2100	0.32	Descendance	252.022
5	2000	2100	0.32	Descendance	240.9531
6	2000	2100	0.32	Descendance	249.9995
7	2000	2100	0.32	Descendance	252.1905
8	2000	2100	0.32	Descendance	242.2763
9	2000	2100	0.32	Descendance	254.9782

As regards a comparison between the two different types of direction, we verified whether the average maximum shear tensile strength of the direction of ascendance was higher than that of the direction of descendance at a significant level of $\alpha = 0.05$.

$$\begin{aligned} \mu_1 &: \text{Direction of Ascendance,} \\ \mu_2 &: \text{Direction of Descendance from the gap} \end{aligned}$$

$$\begin{aligned} H_0 &: \mu_1 - \mu_2 = 0 \\ H_1 &: \mu_1 - \mu_2 > 0 \end{aligned}$$

When $\alpha = 0.05$, the p-value is 0.11. This result was significant and we accepted H1. Therefore, we concluded that the average for the direction of ascendance was higher than it was for the direction of descendance. Table 4.3.3 shows the results of t-Test from the two different directions of welding.

Table 4.3.3 The results of t-Test from the two different directions of welding

	Direction of ascendance	Direction of descendance
Sample size	9	9
Mean	213.35	162.96
90% confidence interval	(187.8, 238.9)	(128.13, 197.79)
Standard deviation	41.219	56.196
Difference between two means	50.392	
90% confidence interval	(9.4758, 91.308)	

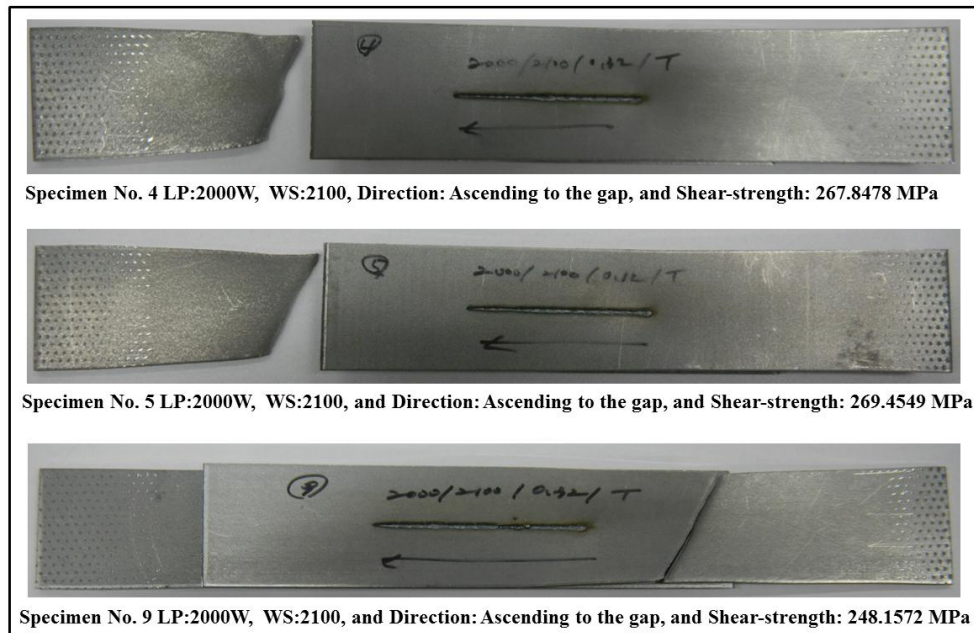


Figure 4.3.2 Specimens breaks at base metals

In addition, when 18 welding runs were performed with both the ascending and the direction of descendances, there were several break areas at the weld bead. Three specimens produced in the direction of ascendance displayed breaks at the base metal, which means that the strength of the weld pool was greater than that of the base metal. Figure 4.3.2 shows the specimens that broke at the base metals.

4.4 Weld microstructure

During the metallographic tests, the test specimens were sampled, mounted, polished, and then etched. In total, 16 samples were tested on the basis of the variations in their gaps. First, each specimen was welded under conditions similar to those used in the previous experiments. Next, the samples were mounted using a hot-mounting press, with each mounted specimen having the weld bead sectioned into five parts, depending on the direction of welding. The specimens were polished in the following three steps:

- 1) Sanding with 180, 320, 600, 800, and 1200 grit papers using a load of 8 N
- 2) Polishing using a 6 μm diamond suspension to remove scratches
- 3) Further polishing using a 1 μm diamond suspension to remove any remaining scratches

Then, the specimens were etched for 2–3 seconds using a Nital solution, which was composed of nitric acid (90%) and ethyl alcohol (10%). After that, the microstructures of the specimens were analyzed using a metallurgical microscope. As mentioned in Chapter 3, two main types of materials were used: 1.4-mm-thick dual-phased galvanized steel sheets and 1.8-mm-thick galvanized steel sheets. Figure 4.4.1 and Figure 4.4.2 show the microstructures of the DP steel and the galvanized steel, respectively. Each figure shows the microstructures of the base metal, the HAZ, and of the weld pool. SGAF590DP is a low-carbon steel that is composed of ferrite and martensite. This steel exhibits better formability and elongation than do other similar carbon steels (Kim 2007).

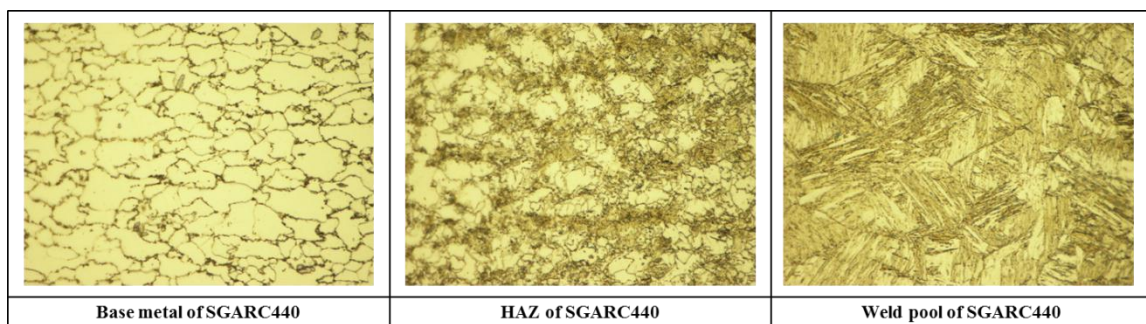


Figure 4.4.1 Microstructures of SGARC440

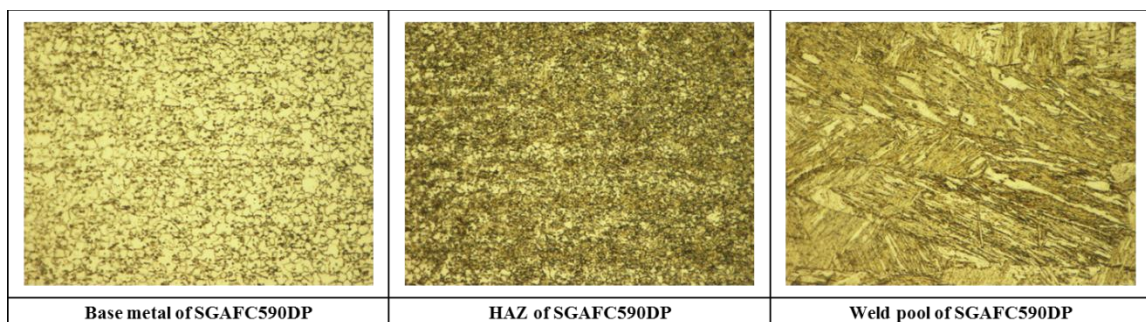


Figure 4.4.2 Microstructures of SGAF590DP

According to Kim and coworkers (2010), when the base material is heated with a laser, the ferrite matrix phase is transformed into austenite, leading to the formation of a final structure that consists of martensite or bainite after cooling. The HAZ, which experiences heating to a greater degree, is heated to temperatures greater than the austenite transformation temperature and is then allowed to cool rapidly. This results in the formation of a structure that is mostly martensite. The weld pool has a fine microstructure and its maximum temperature ranges from 900° to 1100°. As for the weld metal, only a martensite-like structure is observed in it, with the metal not exhibiting properties similar to those of DP steel (Kim et al. 2010).

14 microstructures are showed based on varying gap from 0.1 mm to 0.3 mm. Figure 4.4.3 shows the welded sections based on the direction of weld. On the left side of picture is the direction of Ascendance, and right side of picture is the direction of Descendance.

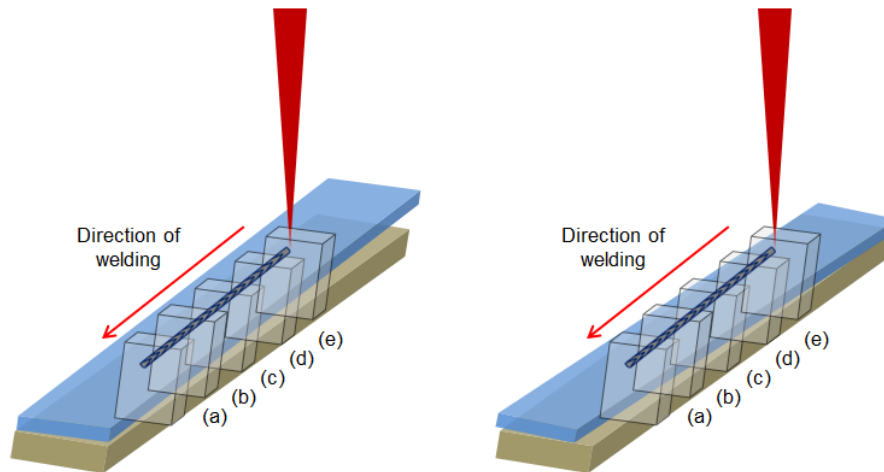


Figure 4.4.3 A schematic drawing of cross-sections arranged on the basis of their directions of welding

As can be seen in Figures 4.4.4–4.4.11, the starting points for laser welding showed full penetration and underfilling. This phenomenon was owing to the fact that the welding speed at the starting positions was lower than the selected constant speed. Therefore, at the starting position, the weld absorbed far more of the input heat energy that it would have at the selected weld speed.

The results of the experiment suggested that the specimens exhibited the highest shear tensile strength when LP was 2000 W and the gaps were 0.3 mm, with the gaps being uniform. On the other hand, the lowest shear tensile strength was noticed when LP was 1400 W and the gaps were 0.1 mm, with the gaps again being uniform. The cross-section exhibiting the lowest shear tensile strength (58.7752 MPa) is shown in Figure 4.4.4 (1). Only a few keyholes were formed in the corresponding specimen, and as can be seen from image (b), a large pore was formed as a result of the evaporation of zinc. This was because the gap was too small to allow the zinc vapors to escape. In addition, the top bead in the case of the specimen with the lowest shear tensile strength was also not stable. Figure 4.4.4 (2) shows the cross-section that exhibited the highest shear tensile strength (269.0149 MPa). It can be seen that all the keyholes were well formed and full penetration took place. In addition, the welded parts between the two materials were also well formed, as can be seen from image (d).

Figure 4.4.5 and Figure 4.4.6 show cross-sections with different welding directions. Images (a)

and (b) in Figure 4.4.5 (3) show weld defects such as pores and cracks because the direction of welding in the case of (3) was from a gap to no gap. This meant that the cross-sections shown in (b) and (a) had limited gap tolerances. In addition, the cross-section in (a) was almost cracked, indicating that the hardness of the welded part was less than that of the base metal and the HAZ. On the other hand, the specimens welded in the direction of ascendance exhibited better weldability than those welded in the direction of descendance. In the case of the specimens welded in the direction of descendance, the shear tensile strength of the cross-sections with a gap was higher (177.5496 MPa) than that of the cross-sections without a gap (90.2105 MPa).

However, for the specimen that had a 0.1 mm gap and exhibited the highest strength, all the cross-sections (those welded in the direction of ascendance as well as those welded in the direction of descendance) contained numerous defects (Figure 4.4.6). Those welded in the direction of descendance (5) (148.8539 MPa) contained a number of large pores, which might have reduced the strength of the cross-sections. In addition, in these cases, the produced zinc vapors could not escape because of the narrow gap. On the other hand, the patterns of those welded in the direction of ascendance (6) were the opposite of those in image (5). This was because the angle of the gaps allowed the zinc vapors to escape along the welding direction. However, the specimens corresponding to either direction did not exhibit high shear tensile strength, because a gap of 0.1 mm did not allow for well-formed weld beads.

Figure 4.4.7 shows cross-sections of the specimen that had a 0.2 mm gap and exhibited the lowest shear tensile strength. The strength of the cross-section in image (7) was 90.2105 MPa. In addition, there were cracks, resulting in the two welded materials not being joined and the cross-section shown in image (a) being broken. However, in comparison, the cross-section in image (8) had no broken parts. This result indicated that the specimens welded in the direction of ascendance exhibited better weld quality. In addition, it was found that a laser with a power of 1400 W was not sufficient to join two sheets of galvanized steel together by welding.

The cross-sections in Figure 4.4.8 exhibited fully penetrative welding. The cross-sections welded in the direction of descendance (9) contained large pores and exhibited a high degree of porosity at the weld pool (a) because of the lack of fusion. In addition, it was evident from the top-view images of the cross-sections of the specimens welded using two different directions that those welded in the direction of descendance (9) contained more spatters and blowholes than did those welded in the direction of ascendance (10). The strength of the cross-section in (9) was 172.0524 MPa and the strength of that in (10) was 237.2453 MPa.

From the specimens that exhibited the lowest shear tensile strength and had a gap of 0.3 mm, a specimen welded in the direction of descendance using a laser with a power of 1400 W was selected

on the basis of the results (Figure 4.4.9). The shear tensile strength of this specimen was 96.5522 MPa, and all its cross-sections exhibited partial penetration. In addition, pores and cracks were noticed throughout the specimen. The cross-section in image (10) had a strength of 176.3852 MPa, whereas that in the reverse direction (9 in Figure 4.4.9) had a strength of 176.3852 MPa of (9). In addition, its gaps were stable from part to part. Finally, the area of the weld pool formed was wider than that in (9).

The cross-sections shown in Figure 4.4.10 exhibited two different maximum shear tensile strengths: the ones shown in (11) had a maximum shear tensile strength of 238.2257 MPa and those in (12) had a maximum shear tensile strength of 237.0161 MPa. The cross-sections shown in images (d) and (e) of (11) were differently shaped from the other cross-sections. This might have been owing to the defocusing of the material, such that the melting started in the center and not from the top bead to the bottom bead.

Figure 4.4.11 shows the optimal regions of the cross-sections that exhibited the highest strength, formed using the steepest ascent method. The images in (1) and (2) both show only sound welded parts. Cracks and pores were not noticed in the parts, and keyholes were formed in all of them. However, the strength of the cross-sections welded in the direction of ascendance was higher than that of those welded in the direction of descendance. This was because welding in the direction of ascendance allowed the part-to-part gap to be reduced when the laser started to melt the upper material.

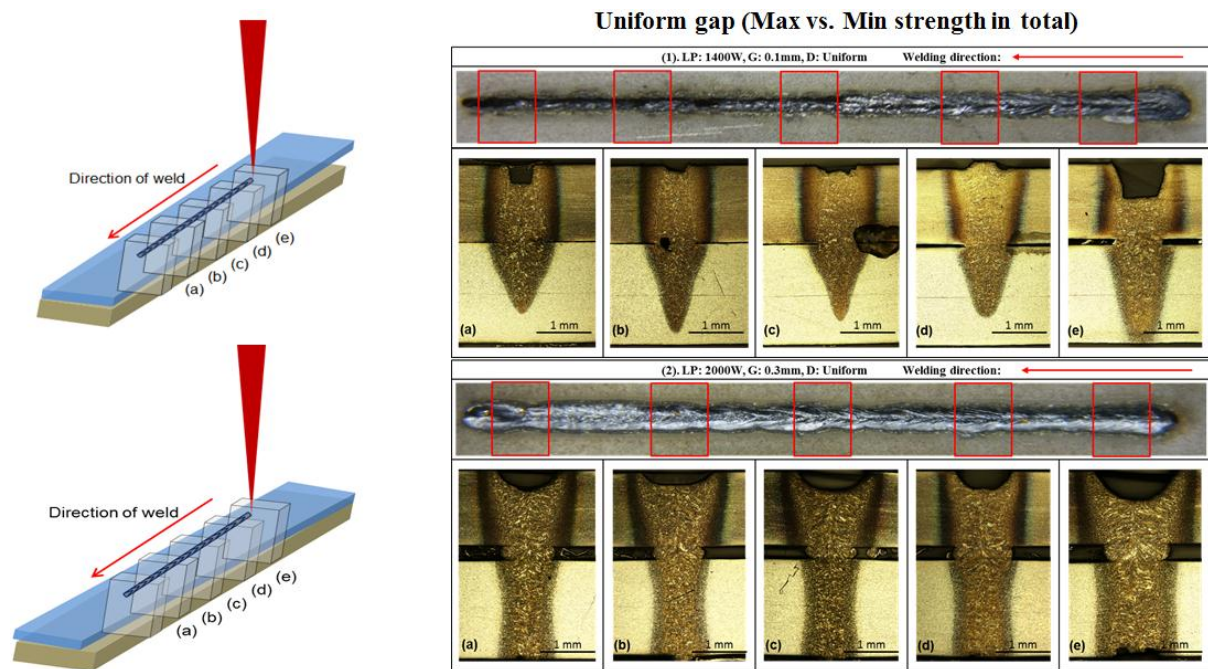


Figure 4.4.4 Cross-sections that had uniform gaps and exhibited the lowest strength (1) and the highest strength (2) in the entire experiment.

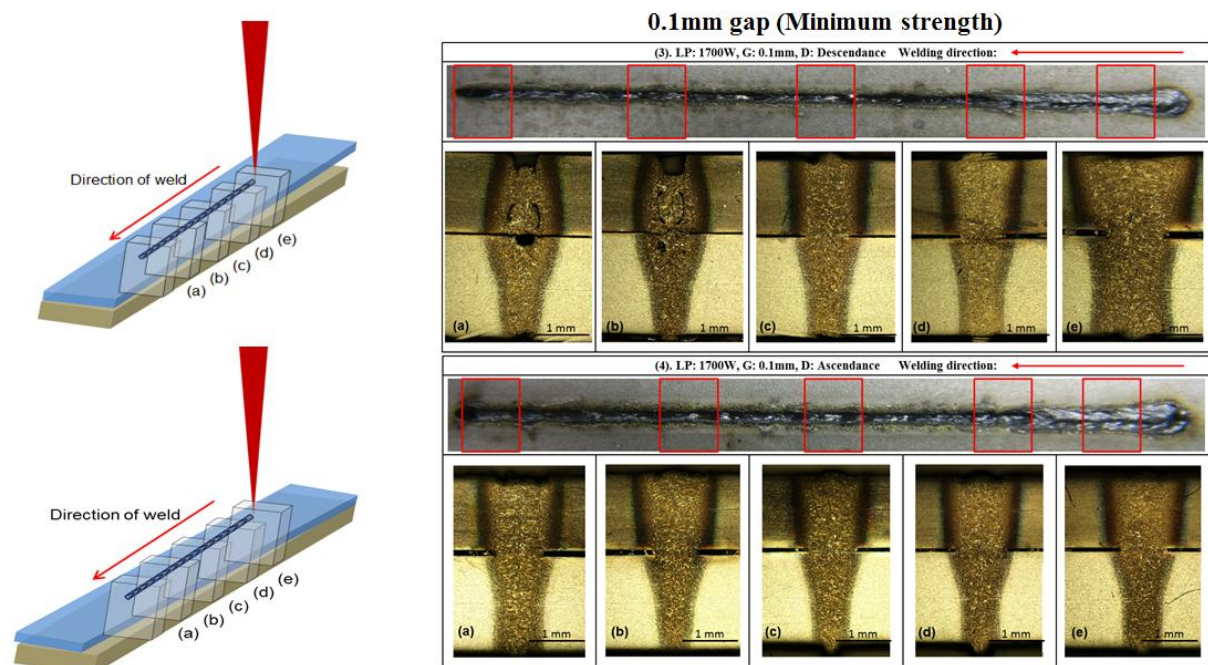


Figure 4.4.5 Cross-sections that had a gap of 0.1 mm and exhibited the lowest strength: (1) Welded in the descendance and (2) ascendance

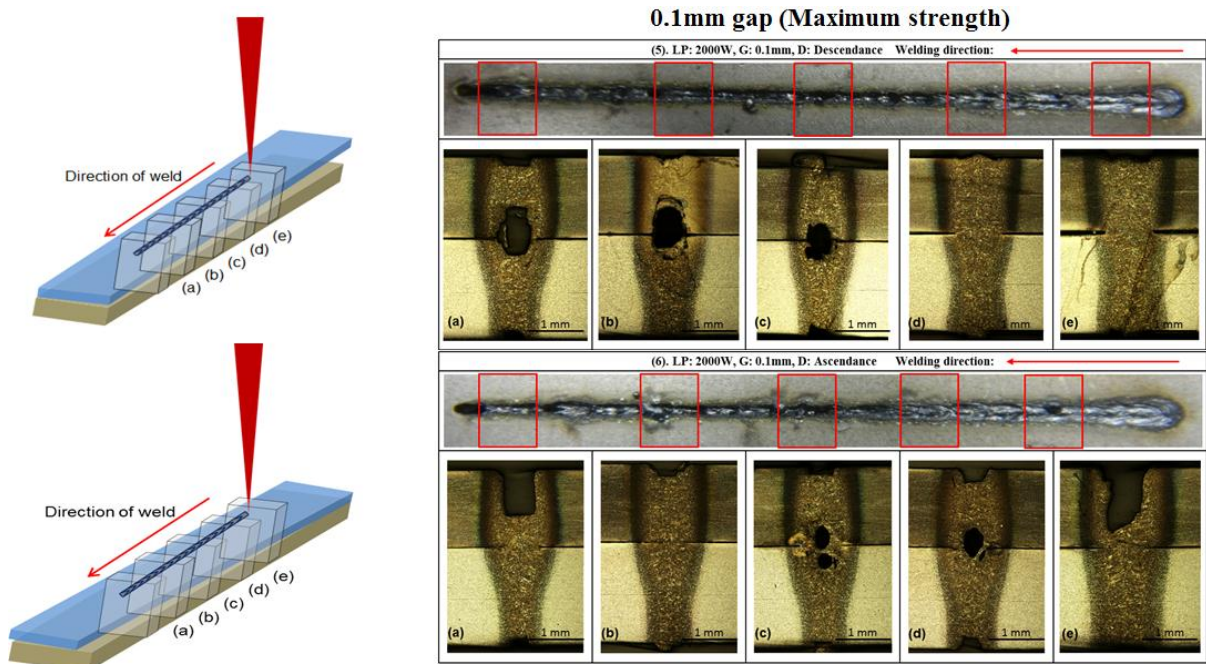


Figure 4.4.6 Cross-sections that had a gap of 0.1 mm and exhibited the highest strength: (1) Welded in the descendance and (2) ascendance

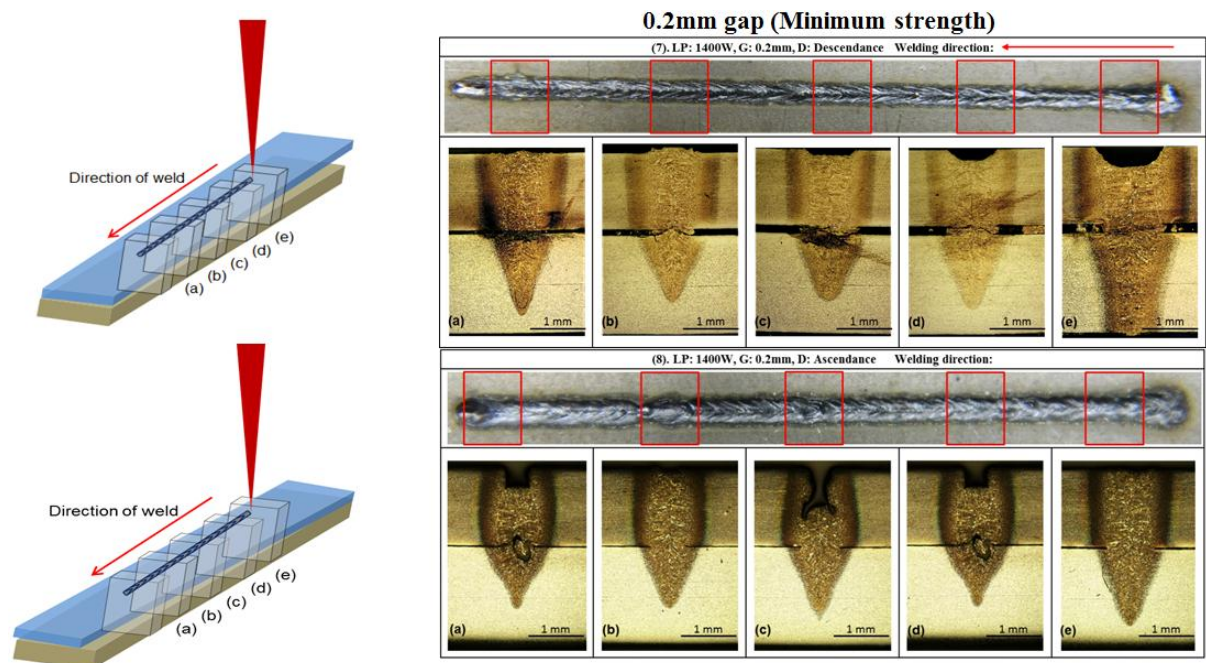


Figure 4.4.7 Cross-sections that had a gap of 0.2 mm and exhibited the lowest strength: (1) Welded in the descendance and (2) ascendance

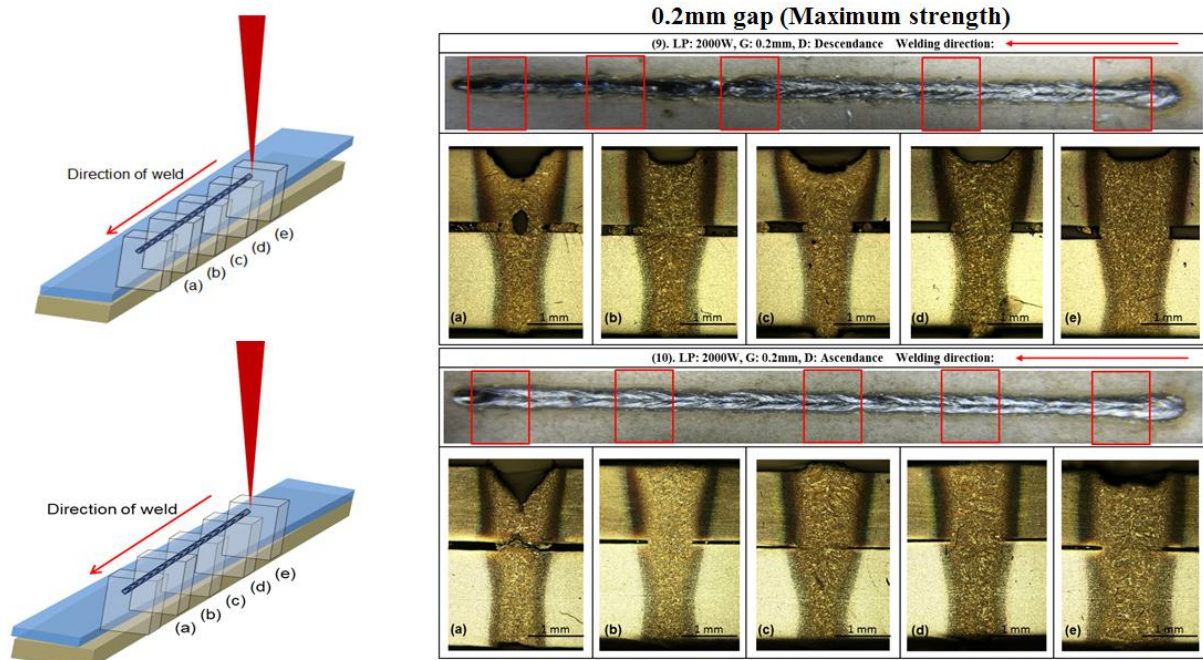


Figure 4.4.8 Figure 4.4.8 Cross-sections that had a gap of 0.2 mm and exhibited the highest strength: (1) Welded in the descendance and (2) ascendance

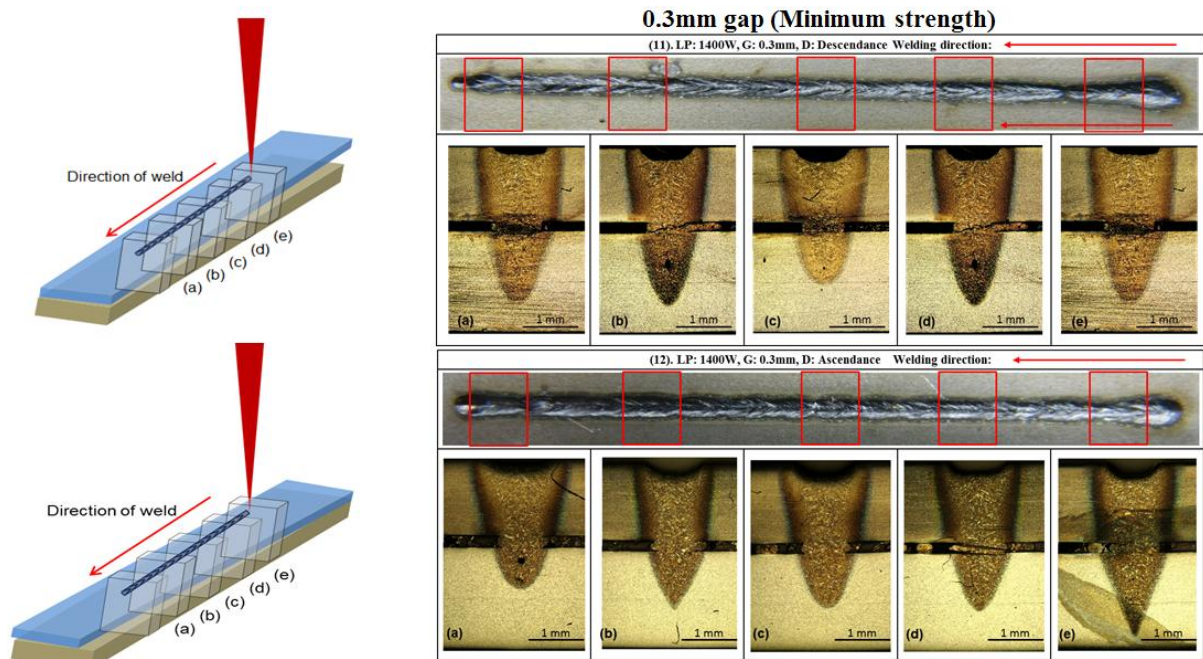


Figure 4.4.9 Cross-sections that had a gap of 0.3 mm and exhibited the lowest strength: (1) Welded in the descendance and (2) ascendance

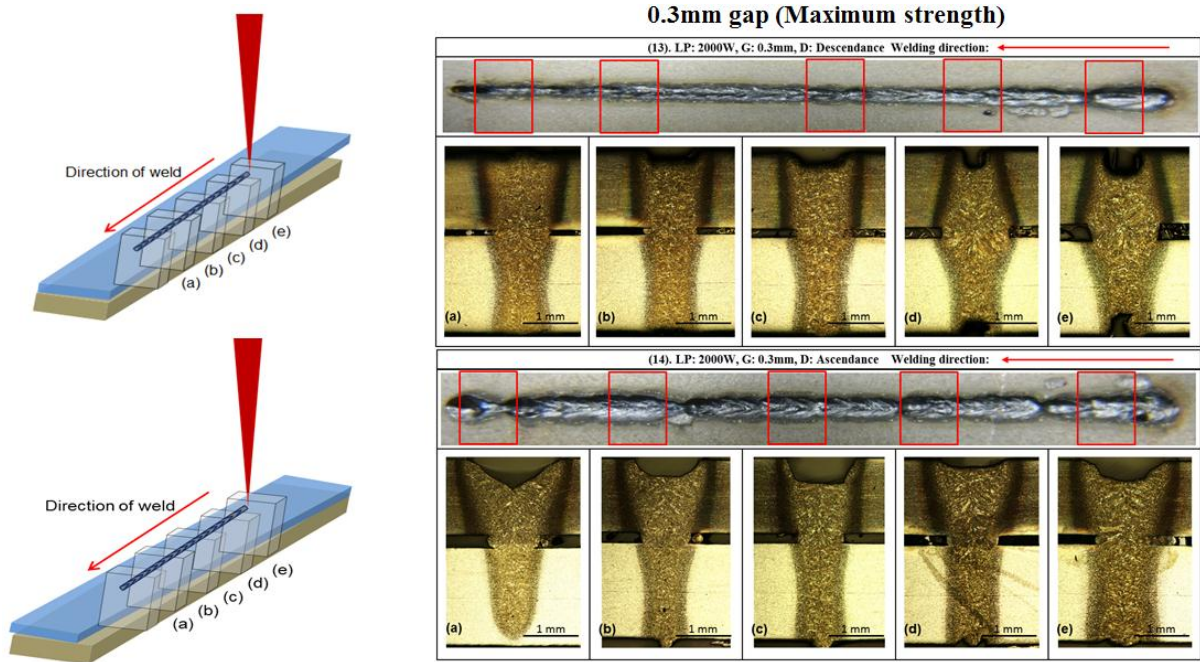


Figure 4.4.10 Cross-sections that had a gap of 0.3 mm and exhibited the highest strength: (1) Welded in the descendance and (2) ascendance

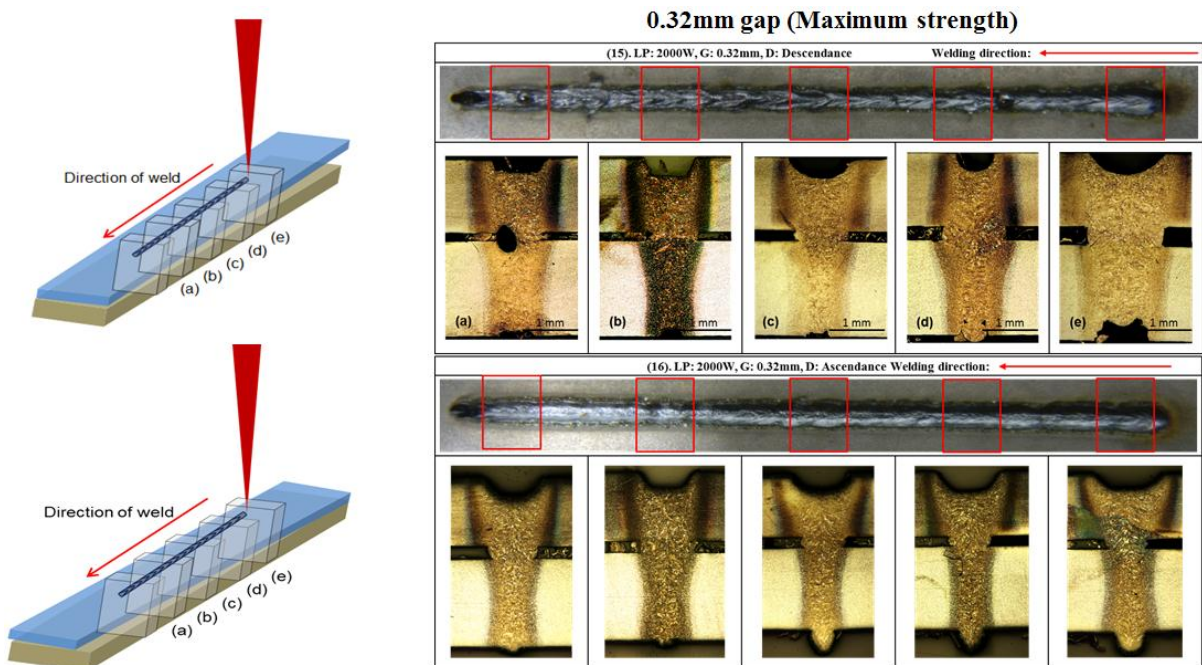
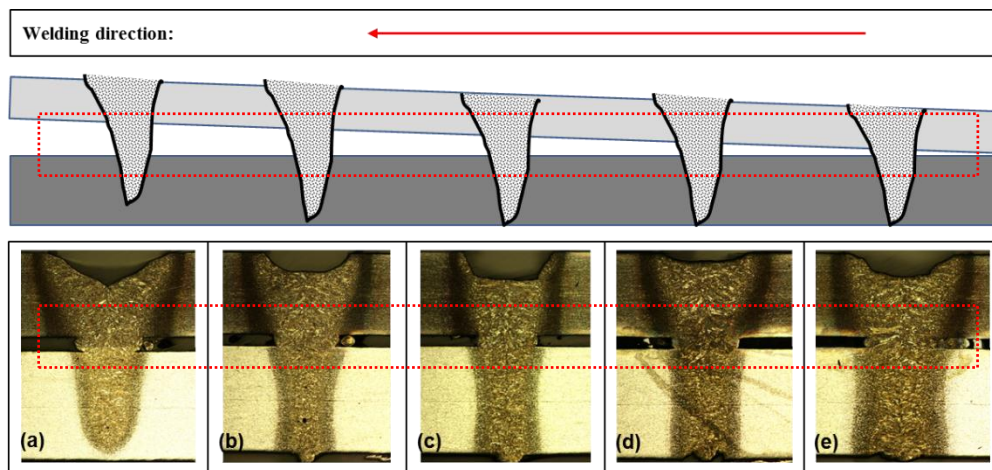
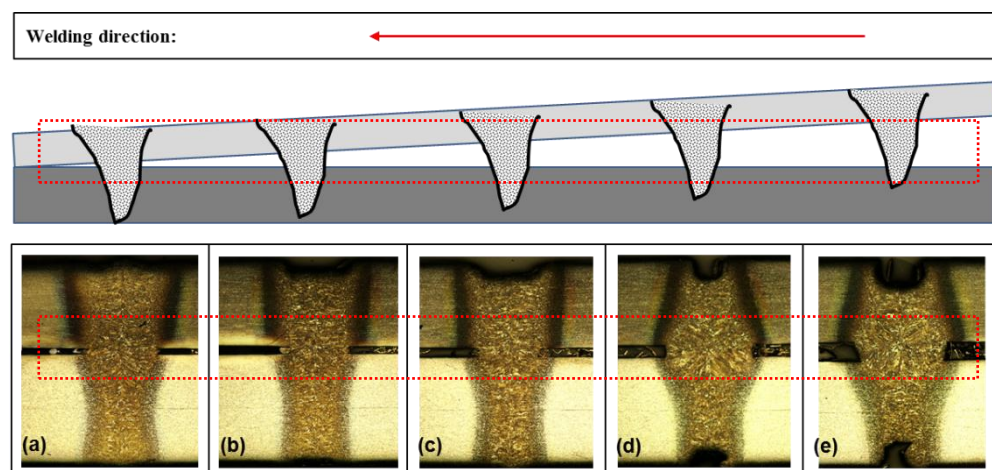


Figure 4.4.11 Cross-sections that had a gap of 0.32 mm and exhibited the highest strength: (1) Welded in the descendance and (2) ascendance

As mentioned in the underlying hypothesis of the study in Chapter 3, it was assumed that the shear tensile strength when the welding was performed in the direction of ascendance was greater than that when it was performed in the direction of descendance. The results of the study also showed that the average shear tensile strength in the case of the direction of ascendance was greater than that in the case of the direction of descendance. However, unlike our hypothesis in the case of cross-sections of the weld beads, the cross-section of the materials welded in the direction of ascendance showed uniform gaps. This indicated that the use of a high-powered laser resulted in the formed weld beads being stable such that the upper part of the weld was pressed against the lower part. On the other hand, the cross-sections of the specimens welded in the direction of descendance exhibited characteristics that were in keeping with our expectations. Figure 4.4.12 shows a comparison of the hypothesized and experimentally determined results.



(1) Cross-sections welded in the Ascendance direction



(2) Cross-sections welded in the Descendance direction

Figure 4.4.12 A comparison of the hypothesized (1) and experimentally determined results (2).

V. Conclusion and future work

In this paper, we have discussed the effect of the part-to-part gap and the direction of welding on the quality of laser welding. In order to simplify the concave or convex model of materials into a linear model, we deliberately used an artificial gap ranging from 0.1 mm to 0.3 mm on one side only. From the results of the experiment, we examined if the direction of a weld is important to ensure the quality of laser lap welding of galvanized steel sheets (1.8 mm thick and 1.4 mm thick). In addition, 3^3 factorial designs with 3 replications were tested, and the steepest ascent method was adopted in order to find region where the optimal strength was achieved. The details of results are summarized as follows:

1. An analysis of variance (ANOVA) with 3 replications, which considered the block effect, showed that all three factors (laser power, part-to-part gap, and direction of weld) have considerable significance, which means that the quality of a weld differs depending on the direction of the weld.
2. When comparing the differences between the two types of directions (ascendance and descendance), the results of a t-Test showed that the average for the direction of ascendance is higher than it is for the direction of descendance.
3. When the steepest ascent method was applied for the direction of ascendance, the maximum parameters are 2000 W of laser power, a welding speed of 2100 mm/min, and a 0.32 mm part-to-part gap.
4. To corroborate the intent of this research, we performed 9 experiments for each welding direction (ascendance and descendance). We also analyzed whether there is difference between the two groups, using a t-Test. The results showed that the average for the direction of ascendance was higher than it was for the direction of descendance.
5. Based on (5), each specimen for maximum strength was in the direction of ascendance, because the angle of the gap allows zinc vapor to escape along the welding direction when the weld pool was welded.
6. When the gap was 0.1 mm and the laser power was 2000 W, there were a number of blowholes, spatters, and pores because the gap was too small to create a channel through which the zinc gas could escape.

7. If the gap is more than 0.32 mm, the welded part of the two materials is weakened, so we need to either increase the laser power or decrease the welding speed.

To summarize the study, we determined that the direction of a weld has a great impact upon the weld quality, unlike the findings of other related studies of controlling the gap between two dissimilar materials. In addition, the shape of the cross-sections obtained also showed that a gap with a constant width can be achieved in the direction of ascendance. The main reason for this result is that a high-power laser plays a role in pressing the gap when the laser source is started from the zero-gap. Moreover, the shear tensile strength produced in the direction of ascendance is greater than it is in the direction of descendance. The reason for this is that the melting pool at the point where the beam is focused cannot be conveyed to the lower part of the materials, owing to the faster cooling of the heat and too great a distance between the two materials.

We have thus determined that there are important relationships between the direction of a weld and the weld quality. A future area that remains to be clarified is if there is also a relationship between different lengths of weld bead and weld quality. The decision regarding the length of the weld bead is also a very important factor that can impact the weld quality. In addition, most materials in industrial manufacturing have randomly different shapes. As a step toward determining the optimal parameters for welding, we need to analyze the process with regard to the randomly varied shapes of materials that are also composed of different raw materials.

Reference

1. Acherjee, B., D. Misra, D. Bose and K. Venkadeshwaran (2009). "Prediction of weld strength and seam width for laser transmission welding of thermoplastic using response surface methodology." *Optics & Laser; Laser Technology* **41**(8): 956-967.
2. Anawa, E. M. and A. G. Olabi (2008). "Using Taguchi method to optimize welding pool of dissimilar laser-welded components." *Optics & Laser Technology* **40**: 379-388.
3. ANSI/AWS (2001). "Standard Welding Terms and Definitions." *ANSI/AWS A3*: 0-89.
4. Benyounis, K. Y., A. G. Olabi and M. S. J. Hashmi (2005). "Effect of laser welding parameters on the heat input and weld-bead profile." *Journal of Materials Processing Technology* **164-165**(0): 978-985.
5. Benyounis, K. Y., A. G. Olabi and M. S. J. Hashmi (2005). "Optimizing the laser-welded butt joints of medium carbon steel using RSM." *Journal of Materials Processing Technology* **164-165**(0): 986-989.
6. Benyounis, K. Y., A. G. Olabi and M. S. J. Hashmi (2008). "Multi-response optimization of CO₂ laser-welding process of austenitic stainless steel." *Optics & Laser Technology* **40**(1): 76-87.
7. Cao, X., W. Wallace, C. Poon and J. P. Immarigeon (2003). "Research and Progress in Laser Welding of Wrought Aluminum Alloys. I. Laser Welding Processes." *Materials and Manufacturing Processes* **18**(1): 1-22.
8. Chen, W., P. Ackerson and P. Molian (2009). "CO₂ laser welding of galvanized steel sheets using vent holes." *Materials and Design* **30**(2): 245-251.
9. Dasgupta, A. and J. Mazumder (2006). A novel method for lap welding of automotive sheet steel using high power CW CO₂ laser. *Proceedings of the 4th International Congress on Laser Advanced Materials Processing*.
10. Defalco, J. (2007). "Hybrid Laser Welding." *Welding journal* **86**(10).
11. Dilthey, U. and L. Stein (2006). "Multimaterial car body design: challenge for welding and joining." *Science and Technology of Welding & Joining* **11**(2): 135-142.
12. Duley, W. W. (1999). *Laser welding*, Wiley.
13. Graham, M. P., D. Hira, H. Kerr and D. Weckman (1996). *Laser welding of Zn-coated sheet steels*. *Proceeding of SPIE: International Society for Optical Engineering*.
14. Gu, H. (2010). "Laser lap welding of zinc coated steel sheet with laser-dimple technology." *Journal of laser applications* **22**: 87.
15. Gunaraj, V. and N. Murugan (1999). "Application of response surface methodology for predicting weld bead quality in submerged arc welding of pipes." *Journal of Materials Processing Technology* **88**(1-3): 266-275.
16. Hafeez, S., N. M. Shaikh, B. Rashid and M. Baig (2008). "Plasma properties of laser-ablated strontium target." *Journal of Applied Physics* **103**: 083117.
17. Han, Y. H. (2010). "Principle and Application of Fiber Lasers." *Optical Science and Technology* **14**(2): 28-33.
18. Heyden, J., K. Nilsson and C. Magnusson, Eds. (1990). *Laser welding of zinc coated steel*. *The Industrial Laser Annual Handbook: 1990 Edition*.
19. Hongping, G. and S. Boris (2011). "Remote Laser Welding of Zinc-Coated Sheetmetal Component in a Lap Configuration Utilizing Humping Effect." *Laser Institute of America* **3**: 380-385.
20. IPG Photonics. "Laser Welding with Ytterbium Lasers ". from <http://www.ipgphotonics.com/>.
21. IPG Photonics (2010). "Operating of IPG Fiber Laser with LaserNet."
22. Jung, J. M., S. H. Baek, C. J. Kim and I. S. Jang (2000). "CW Laser Weld Quality Monitoring in Automobile Industry." *KSLP Conference(2000 Spring Conference)*: 15-19.
23. Kang, H. S., J. M. Jung, K. T. Park, J. O. Kim, J. H. Lee and S. H. Yoo (2006). "Evaluations of laser welding qualities by using plasma sensor." *KSME*: 3065-3068.
24. Kaplan, A. F. H., P. Norman and I. Eriksson (2009). "Analysis of the Keyhole and Weld Pool Dynamics by Imaging Evaluation and Photodiode Monitoring."

25. Katayama, S. (2004). "Laser welding of aluminium alloys and dissimilar metals." *Welding international* **18**(8): 618-625.
26. Katundi, D., A. Tosun-Bayraktar, E. Bayraktar and D. Toueix (2010). "Corrosion behaviour of the welded steel sheets used in automotive industry." *Journal of Achievements in Materials and Manufacturing Engineering Selected full texts* **38**(2): 146-153.
27. Kelkar, G. (2008). "Pulsed Laser Welding." *SOJOM*.
28. Khan, M. M. A., L. Romoli, M. Fiaschi, G. Dini and F. Sarri (2011). "Experimental design approach to the process parameter optimization for laser welding of martensitic stainless steels in a constrained overlap configuration." *Optics & Laser Technology* **43**(1): 158-172.
29. Khorram, A., M. Ghoreishi, M. R. S. Yazdi and M. Moradi (2011). "Optimization of Bead Geometry in CO₂ Laser Welding of Ti 6Al 4V Using Response Surface Methodology." *balance* **3**: 6.
30. Kim, C., J. Choi, M. Kang and Y. Park (2010). "A study on the CO₂ laser welding characteristics of high strength steel up to 1500 MPa for automotive application." *J Achiev Mater Manuf Eng* **39**: 79-86.
31. Kim, C. H. (2006). Laser-arc hybrid welding method and system for zink galvanizing sheet steel. Korea Institute of Patent Information. Korea Institute of Patent Information.
32. Kim, G. Y. (2011). 국내 레이저 용접 산업의 현황과 전망. *Welding journal, Welding Korea*. **3**.
33. Kim, H. K. (2007). "차체용 고장력 강판의 동적 인장 특성 평가." *한국자동차공학 회논문집* **15**(1): 171-176.
34. Kim, I. S. and J. H. Kim (2007). 용접가공일반, 청범출판사.
35. Kim, J. and C. Lee (2010). "Study on the relationship between emission signals and weld defect for in-process monitoring in CO₂ laser welding of Zn-coated steel." *KSME Spring Conference* **34**(10): 1507-1512.
36. Kim, J. D. (2002). "Fundamental Study on the Weld Defects and Real-time Monitoring Method." *KWJS* **20**(1): 26-33.
37. Kim, J. D., J. H. Lee and J. Seo (2011). "Lap Welding of Magnesium Alloy using Nd:YAG Laser." *Korean Society of Laser Processing* **14**(3): 12-16.
38. Kim, K. S., C. H. Jung, I. H. Kim, I. S. Chang and H. B. Lee (2005). "Development of remote welding system using fiber laser." *Korea Society of Laser Processing* **8**(Journal of KSLP Vol.8 No.3): 27-30.
39. Kim, K. Y. (2011). Welding and cutting, laser industry information Korea. *Welding Korea, Metal Network Korea*. **9**: 170-181.
40. Klingbeil, K. (2006). "What you need to know about remote laser welding." *Welding journal* **85**(8): 44-46.
41. Larsson, L. O., N. Palmquist, V. Cars and J. K. Larsson (2000). "High quality aluminium welding—a key factor in future car body production." *Svetsaren* **54**(2): 17-24.
42. Li, X., S. Lawson, Y. Zhou and F. Goodwin (2007). "Novel technique for laser lap welding of zinc coated sheet steels." *Journal of laser applications* **19**: 259.
43. Mazumder, J., A. Dasgupta and M. Bembenek (2002). Alloy based laser welding, Google Patents.
44. Montgomery, D. C. (2008). Design and analysis of experiments, John Wiley & Sons Inc.
45. Myers, R. H., D. C. Montgomery and C. M. Anderson-Cook (2009). Response surface methodology: process and product optimization using designed experiments, John Wiley & Sons Inc.
46. Olabi, A. G., K. Y. Benyounis and M. S. J. Hashmi (2007). "Application of Response Surface Methodology in Describing the Residual Stress Distribution in CO₂ Laser Welding of AISI304." *Strain(An International Journal for Experimental Mecahnics)* **43**(1): 37-46.
47. Olabi, A. G., G. Casalino, K. Y. Benyounis and M. S. J. Hashmi (2006). "An ANN and Taguchi algorithms integrated approach to the optimization of CO₂ laser welding." *Advances in Engineering Software* **37**(10): 643-648.

48. Olabi, A. G., G. Casalino, K. Y. Benyounis and A. Rotondo (2007). "Minimisation of the residual stress in the heat affected zone by means of numerical methods." *Materials & Design* **28**(8): 2295-2302.
49. Ozaki, H., M. Kutsuna, S. Nakagawa and K. Miyamoto (2010). "Laser roll welding of dissimilar metal joint of zinc coated steel to aluminum alloy." *Journal of laser applications* **22**: 1.
50. Pan, L. K., C. C. Wang, Y. Ching Hsiao and K. Chyn Ho (2004). "Optimization of Nd:YAG laser welding onto magnesium alloy via Taguchi analysis." *Optics & Laser Technology* **37**: 33-42.
51. Pan, L. K., C. C. Wang, Y. C. Hsiao and K. C. Ho (2005). "Optimization of Nd: YAG laser welding onto magnesium alloy via Taguchi analysis." *Optics & Laser Technology* **37**(1): 33-42.
52. Park, H., S. Rhee and D. Kim (2001). "A fuzzy pattern recognition based system for monitoring laser weld quality." *Measurement Science and Technology* **12**(8): 1318.
53. Park, Y. H. (2010). "Weld Formability Evaluation and Formability Estimation Model Development in Aluminum Laser Welding." *Korea Society of Laser Processing Conference* **13**(3): 7-12.
54. Pennington, E. J. (1987). Laser welding of galvanized steel, Google Patents.
55. Sergio, S. R., A. G. Roberto, B. José, R. Fernando, M. Luis and P. José (2010). "Laser welding defects detection in automotive industry based on radiation and spectroscopical measurements." *The International Journal of Advanced Manufacturing Technology* **49**(1): 133-145.
56. Shao, J. and Y. Yan (2005). Review of techniques for on-line monitoring and inspection of laser welding, IOP Publishing.
57. Sibillano, T., A. Ancona, V. Berardi and P. M. Lugarà (2009). "A Real-Time Spectroscopic Sensor for Monitoring Laser Welding Processes." *Sensors* **9**(5): 3376-3385.
58. Son, J. S., K. D. Lee and S. B. Park (1999). "Monotoring Secheme of Laser Welding Interior Defects Using Neural Network." *Korean Society of Laser Processing* **2**(3): 19-31.
59. Steen, W. M. and J. Mazumder (2010). Laser material processing, Springer Verlag.
60. Sun, Z. and M. Kuo (1999). "Bridging the joint gap with wire feed laser welding." *Journal of Materials Processing Technology* **87**(1): 213-222.
61. Tanco, M., L. Ilzarbe, E. Viles and M. J. Alvarez (2008). "Applying design of experiments to improve a laser welding process." *Journal of Engineering Manufacture* **222**:1035.
62. Tian, J. and Z. N. Zhang (2012). "The De-Gassing Evaluation with Full Penetration for Remote Laser Welding of Zinc Coated Sheet Metal." *Advanced Materials Research* **496**: 272-275.
63. Tzeng, Y. (1999). "Pulsed Nd: YAG laser seam welding of zinc-coated steel." *WELDING JOURNAL-NEW YORK-* **78**: 238.
64. Tzeng, Y. F. (2000). "Process characterisation of pulsed Nd: YAG laser seam welding." *The International Journal of Advanced Manufacturing Technology* **16**(1): 10-18.
65. Wu, Q., J. Gong, G. Chen and L. Xu (2008). "Research on laser welding of vehicle body." *Optics & Laser Technology* **40**(2): 420-426.
66. Xie, J. (2002). "Dual beam laser welding." *Welding journal* **81**(10): 223s-230s.
67. Yang, S., B. Carlson and R. Kovacevic (2011). "Laser Welding of High-Strength Galvanized Steels in a Gap-Free Lap Joint Configuration under Different Shielding Conditions." *Welding journal* **90**: 8-18.
68. Yoo, Y. S., K. H. Kim and Y. B. Jung (2006). "A study on the Optimization for the Blasting Process of Glass by Taguchi Method." *KSIE Conference*: 195-202.
69. Zhao, H., D. White and T. DebRoy (1999). "Current issues and problems in laser welding of automotive aluminium alloys." *International materials reviews* **44**(6): 238-266.
70. Zhao, Y., Y. Zhang, W. Hu and X. Lai (2012). "Optimization of laser welding thin-gage galvanized steel via response surface methodology." *Optics and Lasers in Engineering*.

Appendix

In order to find out the optimal laser welding parameters, a new extra work has been carried out and the detailed steps are categorized as follows:

1. Welding speed was re-set up in order to satisfy the full penetration of 3.2 mm of thickness.
2. The range of welding speed was from 1400 mm/min to 2100 mm/min. However, 1400 to 1500 mm/min for welding speed showed a lot of spatters and through and through holes. In addition, 1700 to 2100 mm/min for welding speed could not make the full penetrations.
3. Part-to-part gap was designated to 0.25mm and compared to the 0.32mm gap.
4. Each group (0.25 mm of gap and 0.32mm of gap) has 20 specimen and 5 representative conditions of specimen were selected for the tensile test. Table 1 shows the maximum tensile strength as compared to the direction of welding and welding speed.
5. Cross-sections were observed for mainly three parts.

No	LP	WS	G	D	Tensile Strength	
1	2000	1600	0.25	Ascendance	260.1166	
2	2000	1600	0.25	Ascendance	259.7256	
3	2000	1600	0.25	Ascendance	266.793	
4	2000	1600	0.25	Ascendance	268.957	
5	2000	1600	0.25	Ascendance	260.9692	263.3123
6	2000	1600	0.32	Ascendance	267.4579	
7	2000	1600	0.32	Ascendance	266.0994	
8	2000	1600	0.32	Ascendance	268.1326	
9	2000	1600	0.32	Ascendance	263.0384	
10	2000	1600	0.32	Ascendance	254.8438	263.9144
11	2000	1600	0.25	Descendance	251.5395	
12	2000	1600	0.25	Descendance	254.0729	
13	2000	1600	0.25	Descendance	244.0806	
14	2000	1600	0.25	Descendance	233.0495	
15	2000	1600	0.25	Descendance	246.7269	245.8939
16	2000	1600	0.32	Descendance	256.3905	
17	2000	1600	0.32	Descendance	251.1241	
18	2000	1600	0.32	Descendance	246.8589	
19	2000	1600	0.32	Descendance	233.1691	
20	2000	1600	0.32	Descendance	249.9437	247.4972

Results

1. Based on the same directions (ascendance and descendance), the tensile strength of 0.25 mm gap and 0.32mm gap has almost same values (Table 1).
2. Under the same directions, tensile strength of ascendance welding direction has higher than the descendance welding direction.
3. From the cross sections of specimen (Figure 1), 2000W of laser power, 1600 mm/min of welding speed, 0.32 mm of gap, and ascendance of welding direction as a new experiment showed a better quality of weld because width of weld bead become wider due to the slower welding speed as compared to the previous experiment (Figure 2).
4. From the cross sections of specimen (Figure 3), 2000W of laser power, 1600 mm/min of welding speed, 0.32 mm of gap, and descendance of welding direction as a new experiment showed an underfill because of wider gap between two sheets. However, when following to the descendance welding direction, keyhole of the cross section became stable as compared to the previous experiment (Figure 4).
5. When welding with 0.25 mm gap, the conditions of cross sections in Figure 5 were better than the Figure 1. In addition, in terms of tensile strength, ascendance welding direction has stronger value than the descendance welding directions.

Conclusion

When changing the welding speed as 1600 mm/min, wider bead width was formed as the spot size become wider, and the tensile strength of ascendance welding direction showed higher than the descendance welding direction. In addition, 0.25mm of gap has better conditions of cross sections as compared to the 0.32mm of gap.

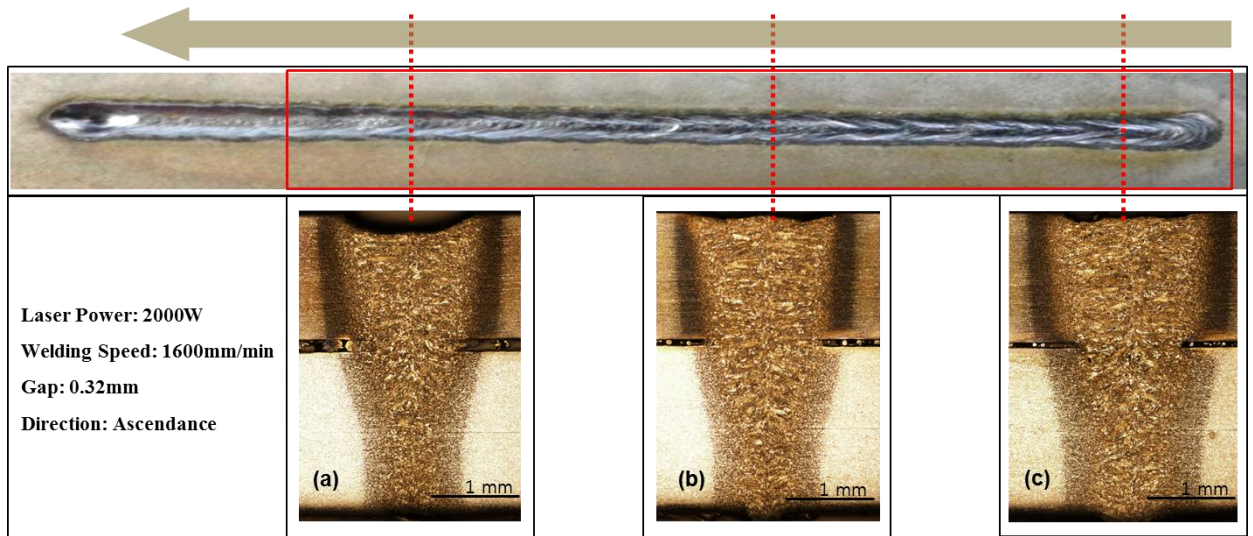


Figure 2: Laser Power: 2000W, Welding Speed: 1600mm/min, Gap: 0.32mm, Direction: Ascendance

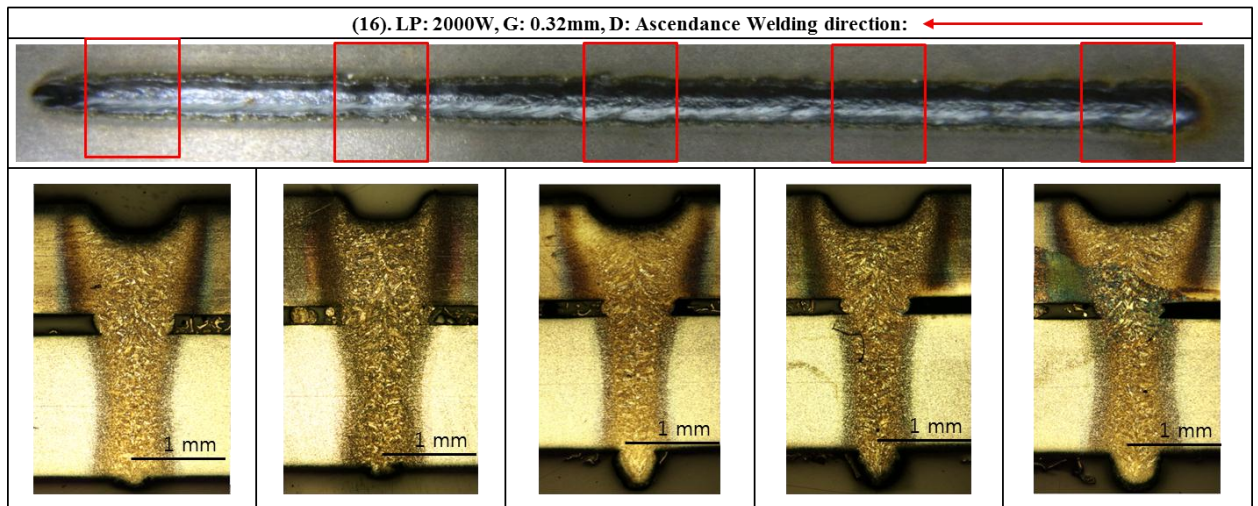


Figure 3: Laser Power: 2000W, Welding Speed: 2100mm/min, Gap: 0.32mm, Direction: Ascendance

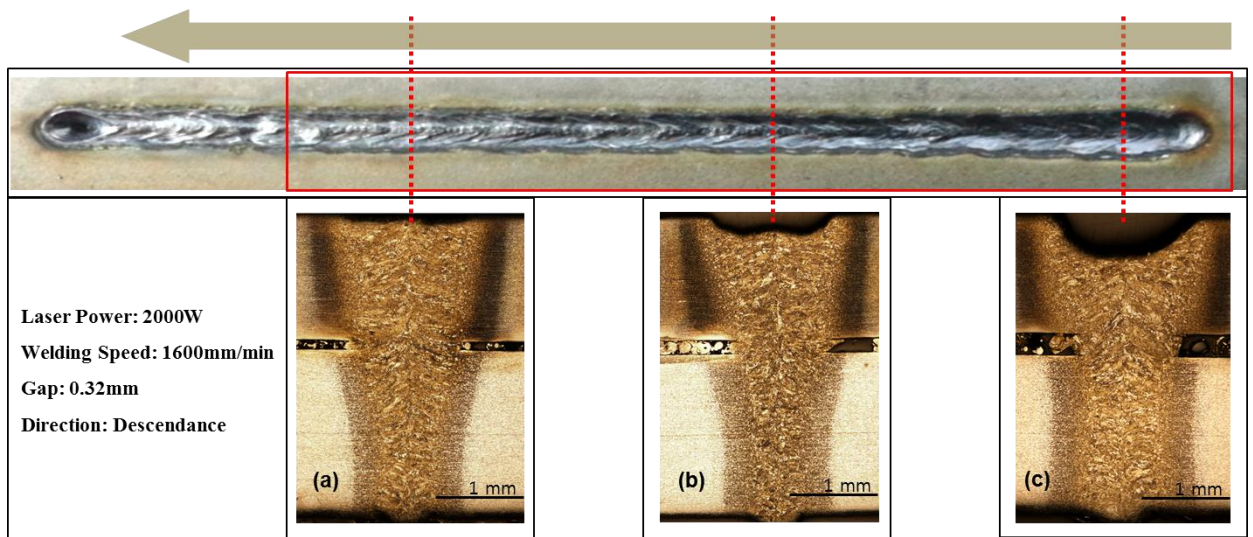


Figure 4: Laser Power: 2000W, Welding Speed: 1600mm/min, Gap: 0.32mm, Direction: Descendance

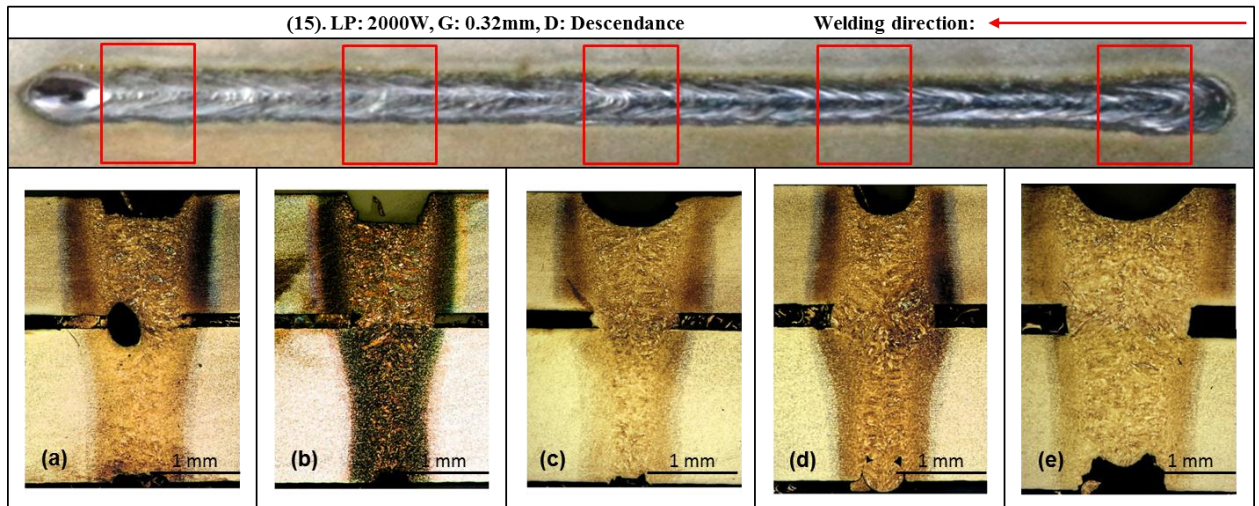


Figure 5: Laser Power: 2000W, Welding Speed: 2100mm/min, Gap: 0.32mm, Direction: Descendance

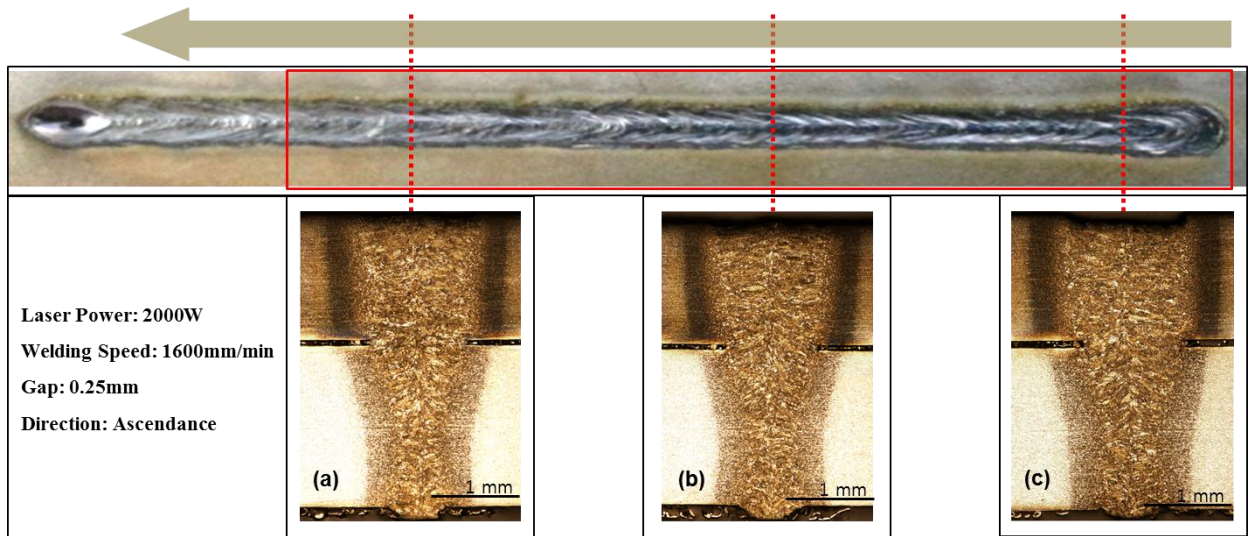


Figure 6: Laser Power: 2000W, Welding Speed: 1600mm/min, Gap: 0.25mm, Direction: Ascendance

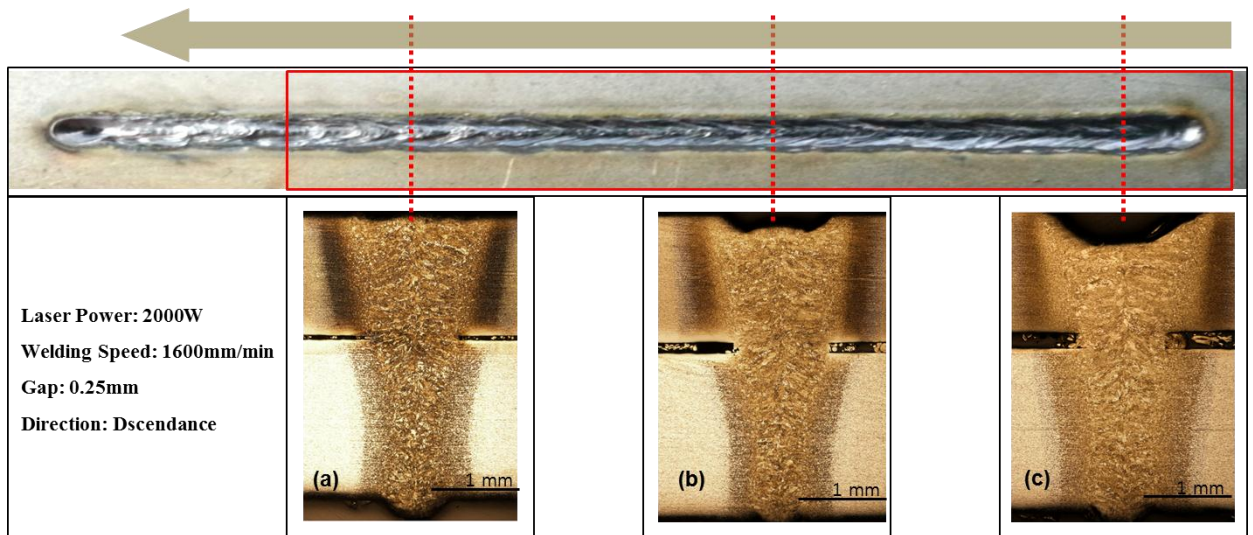


Figure 7: Laser Power: 2000W, Welding Speed: 1600mm/min, Gap: 0.25mm, Direction: Descendance

Acknowledgement

I would like to express my sincere gratitude to my advisor Prof. Duck-Young KIM for the continuous support of my Master degree. His guidance helped me in all the time of research and writing of this thesis. I could not have imagined having a better advisor and mentor for my graduate study.

Besides my advisor, I would like to thank the rest of my thesis committee: Prof. Hyung-Son KI, and Prof. Nam-Hun KIM, for their encouragement, insightful comments, and hard questions.

My sincere thanks also goes to Prof. Jae-Kyun KIM and Prof. Dae-Won Lee for suggesting me to consider graduate studies in UNIST.

I thank my fellow labmates: Amit Kumar Sinha, Prerna Swati, and Su Jung Back, most importantly Yang-Ji Lee, for supporting and encouraging me during Master's study. Amit, Prerna, and Su Jung always help me to complete my thesis. And I always thank U-CIM Lab members: Hae-seung Park, Young-Gwang Oh, Moise Busogi, and A-rm. Also, I thank my fellows in University of Ulsan. They always encouraged me to make the best choice whenever I faced with problems.

I would like to thank my parents and my older brother. They always supported and believed me. I always pray that my mother would recover from her illness and my older brother will finish his Master's degree at U-Penn.

Last but not the least, my lovely fiancé Bo-Ri Choi, I always thank for her patience and wisdom. And I wish her graduate work also will be successful with great results.